# EFFECT OF BLAST ON BUILDINGS

A thesis submitted

In partial fulfillment of the requirements for

the award of the degree of

**MASTERS OF ENGINEERING**

**IN**

**STRUCTURAL ENGINEERING**

Submitted by

**RAVI KUMAR**

**(ROLL NO.820922003)**

UNDER THE GUIDANCE OF:

**Dr Naveen Kwatra**

Head and Associate Professor

Deptt. Of Civil Engineering,

**Thapar University,Patiala**


THAPAR UNIVERSITY, PATIALA

## DECLARATION

I hereby declare that the thesis entitled "**Effects of blast on buildings**"is an authentic record of my own work carried out as requirements for the award of degree M.E. (Structures) at Thapar Institute of Engineering and Technology (Deemed University), Patiala, under the guidance of Dr. Naveen Kwatra, Associate Professor and Head of Department of Civil Engineering.

Date : _____

Place: Patiala

Ravi Kumar

Roll No. 820922003

## CERTIFICATE

This si to certify that the theisis entitled **"Effects of Blast on Building"** being submitted by **Ravi Kumar Roll No.820922003** in partial fulfillment for the award of degree of **Masters of Engineering in Structural Engineering** at **Thapar University,Patiala** is a bonofide work carried out by him under my guidance and that no part of this theisis has been submitted for the award of any other degree.

15/7/13

Dr. Naveen Kwatra

(Associate Professor and Head of Department)

**Countersigned by:**

15/7/13

**(Dr. Naveen Kwatra)**

Chairman,Board of Studies,

Department of Civil Engineering

Thapar University, Patiala.

**(Dr. S. K. Mohapatra)**

Dean, Academics Affairs

Thapar University, Patiala

# ACKNOWLEDGEMENT

I take this opportunity to express my sincere gratitude to **Dr. Naveen Kwatra, Head and Associate Professor, Civil Engineering Department, Thapar University, Patiala**, for giving me the opportunity of doing my thesis work under his guidance. It is my proud privilege to express regards and sincere gratitude for his constant supervision, valuable suggestions, patient listening of my ideas and also suggesting new ways for implementing my ideas by his expert guidance throughout my work.

I also take this opportunity to thank to the entire faculty and staff of **Civil Engineering Department,** Thapar University, Patiala, for their help, inspiration and moral support, which went a long way in successfully completion of this report.

Finally, I would like to express my deepest gratitude to **family**, without whom I am nothing, to provide me great opportunities, everlasting support, big encouragement and lots of love.

**Ravi Kumar**

**(Roll No. 820922003)**

# ABSTRACT

In the past few decades considerable emphasis has been given to problems of blast and earthquake. The earthquake problem is rather old, but most of the knowledge on Effects of Blast on Buildings has been accumulated during the past fifty years.

Due to different accidental or intentional events, the behavior of structural components subjected to blast loading has been the subject of considerable research effort in recent years. Conventional structures, particularly that above grade, normally are not designed to resist blast loads; and because the magnitudes of design loads are significantly lower than those produced by most explosions, conventional structures are susceptible to damage from explosions.

In this Study, the blast loading was modeled using standard equations suggested by Smith et al. (1994 & 2001). Then influence of blast loading with variation of scale distanced was investigated.

The basic objective of the investigation is to study the effect of blasting loading on the bench mark problem of building by using ETABS as helping software for modeling the structure as well the performance of structure due to blast pressure was investigated by the standard equations apart from that influence of structural parameter investigated due blast pressure.

## LIST OF CONTENTS

# CHAPTER 1

# INTRODUCTION

## 1.1 General

An explosion is an extremely rapid release of energy in the form of light, heat, sound, and a shock wave. The shock wave consists of highly compressed air that wave-reflects off the ground surface to produce a hemispherical propagation of the wave that travels outward from the source at supersonic velocities.

Extensive studies during the last five decades have shown that short-duration high-magnitude loading conditions significantly influence structural response. Explosive loads are typically applied to structures at rates approximately 1000 times faster than earthquake-induced loads. The corresponding structural response frequencies can be much higher than those induced by conventional loads. Furthermore, short-duration dynamic loads often exhibit strong spatial and time variations, resulting in sharp stress gradients in the structures. It is known that high strain rates also affect the strength and ductility of structural materials, the bond relationships for reinforcement, the failure modes, and the structural energy absorption capabilities.

Due to different accidental or intentional events, related to important structures all over the world, explosive loads have received considerable attention in recent years. The design and construction of public buildings to provide life safety in the face of explosions is receiving renewed attention from structural engineers. Such concern arose initially in response to air attacks during World War II, it continued through the Cold War and more recently this concern has grown with the increase of terrorism worldwide. For many urban settings, the proximity to unregulated traffic brings the terrorist threat to or within the perimeter of the building.

For these structures, blast protection has the modest goal of containing damage in the immediate vicinity of the explosion and the prevention of progressive collapse. In this sense, computer programs simulations could be very valuable in testing a wide range of building types and structural details over a broad range of hypothetical events.

In the past few decades considerable emphasis has been given to problems of blast and earthquake. The earthquake problem is rather old, but most of the knowledge on this subject has been accumulated during the past fifty years. The blast problem is rather new; information about the development in this field is made available mostly through publication

of the Army Corps of Engineers, Department of Defense, U.S. Air Force and other governmental office and public institutes. Much of the work is done by the Massachusetts Institute of Technology, The University of Illinois, and other leading educational institutions and engineering firms.

Due to different accidental or intentional events, the behavior of structural components subjected to blast loading has been the subject of considerable research effort in recent years. Conventional structures, particularly that above grade, normally are not designed to resist blast loads; and because the magnitudes of design loads are significantly lower than those produced by most explosions, conventional structures are susceptible to damage from explosions. With this in mind, developers, architects and engineers increasingly are seeking solutions for potential blast situations, to protect building occupants and the structures.

**1.2 Classification of Explosions**

1- Physical

2- Nuclear or chemical events.

In physical explosions, energy may be released from the catastrophic failure of a cylinder of compressed gas, volcanic eruptions or even mixing of two liquids at different temperatures.

In a nuclear explosion, energy is released from the formation of different atomic nuclei by the redistribution of the protons and neutrons within the interacting nuclei, whereas the rapid oxidation of fuel elements (carbon and hydrogen atoms) is the main source of energy in the case of chemical explosions.

The type of burst mainly classified as

a. Air burst
b. High altitude burst
c. Under water burst
d. Underground burst
e. Surface burst

The discussion in this section is limited to air burst or surface burst. This information is then used to determine the dynamic loads on surface structures that are subjected to such blast pressures and to design them accordingly. It should be pointed out that surface structure

cannot be protected from a direct hit by a nuclear bomb; it can however, be designed to resist the blast pressures when it is located at some distance from the point of burst.

Explosive materials can be classified according to their physical state as

1- Solids

2- Liquids or Gases.

Solid explosives are mainly high explosives for which blast effects are best known. They can also be classified on the basis of their sensitivity to ignition as: secondary or primary explosive.

The latter is one that can be easily detonated by simple ignition from a spark, flame or impact. Materials such as mercury fulminate and lead azide are primary explosives.

Secondary explosives when detonated create blast (shock) waves which can result in widespread damage to the surroundings.

The detonation of a condensed high explosive generates hot gases under pressure up to 300 kilo bar and a temperature of about 3000-4000C°. The hot gas expands forcing out the volume it occupies. As a consequence, a layer of compressed air (blast wave) forms in front of this gas volume containing most of the energy released by the explosion. Blast wave instantaneously increases to a value of pressure above the ambient atmospheric pressure. This is referred to as the side-on overpressure that decays as the shock wave expands outward from the explosion source.

After a short time, the pressure behind the front may drop below the ambient pressure.

During such a negative phase, a partial vacuum is created and air is sucked in. This is also accompanied by high suction winds that carry the debris for long distances away from the explosion source.

**1.3 Types of threats**

a- Vehicle weapon

b- Hand-delivered weapon

Airborne Chemical, Biological, and Radiological threat:

a- Large-scale, external, air-borne release

b- External release targeting building

c- Internal release

Although it is possible that the dominant threat mode may change in the future, bombings have historically been a favorite tactic of terrorists.

Ingredients for homemade bombs are easily obtained on the open market, as are the techniques for making bombs. Bombings are easy and quick to execute. Finally, the dramatic component of explosions in terms of the sheer destruction they cause creates a media sensation that is highly effective in transmitting the terrorist's message to the public.

The threat for a conventional bomb is defined by two equally important elements, the bomb size, or charge weight W, and the standoff distance R between the blast source and the target. For example, the blast occurred at the basement of World Trade Centre in 1993 has the charge weight of 816.5 kg TNT. The Oklahoma bomb in 1995 has a charge weight of 1814 kg at a standoff of 4.5m (Longinow, 1996). As terrorist attacks may range from the small letter bomb to the gigantic truck bomb as experienced in Oklahoma City, the mechanics of a conventional explosion and their effects on a target must be addressed.

The destructive action of nuclear weapon is much more severe than that of a conventional weapon and is due to blast or shock. In a typical air burst at an altitude below 100,000 ft. an approximate distribution of energy would consist of 50% blast and shock, 35% thermal radiation, 10% residual nuclear radiation and 5% initial nuclear radiation .

The sudden release of energy initiates a pressure wave in the surrounding medium, known as a shock wave as shown in Fig. 1.1 (a). When an explosion takes place, the expansion of the hot gases produces a pressure wave in the surrounding air. As this wave moves away from the centre of explosion, the inner part moves through the region that was previously compressed and is now heated by the leading part of the wave. As the pressure waves moves with the velocity of sound, the temperature is about 3000o-4000oC and the pressure is nearly 300 kilobar of the air causing this velocity to increase. The inner part of the wave starts to move faster and gradually overtakes the leading part of the waves. After a short period of time the pressure wave front becomes abrupt, thus forming a shock front some what similar to Fig. 1.1(b). The maximum overpressure occurs at the shock front and is called the peak overpressure. Behind the shock front, the overpressure drops very rapidly to about one-half the peak overpressure and remains almost uniform in the central region of the explosion.

An expansion proceeds, the overpressure in the shock front decreases steadily; the pressure behind the front does not remain constant, but instead, fall off in a regular manner.

After a short time, at a certain distance from the centre of explosion, the pressure behind the shock front becomes smaller than that of the surrounding atmosphere and so called negative-phase or suction.

The front of the blast waves weakens as it progresses outward, and its velocity drops towards the velocity of the sound in the undisturbed atmosphere. This sequence of events is shown in Fig. 1.1(c), the overpressure at time t1, t2…..t6 are indicated. In the curves marked t1 to t5, the pressure in the blast has not fallen below that of the atmosphere. In the curve t6 at some distance behind the shock front, the overpressure becomes negative. This is better illustrated in Fig.1.2 (a). Fig.1.2 (a) The variation of overpressure with distance at a given time from centre of explosion.Fig.1.2 (b) Variation of overpressure with distance at a time from the explosion. Fig.1.2(c) Variation of dynamic pressure with distance at a time from the explosion. The time variation of the same blast wave at a given distance from the explosion is shown in Fig 1.2(b); to indicate the time duration of the positive phase and also the time at the end of the positive phase. Another quantity of the equivalent importance is the force that is developed from the strong winds accompanying the blast wave known as the dynamic pressure; this is proportional to the square of the wind velocity and the density of the air behind the shock front. Its variation at a given distance from the explosion is shown in Fig.1.2(c).

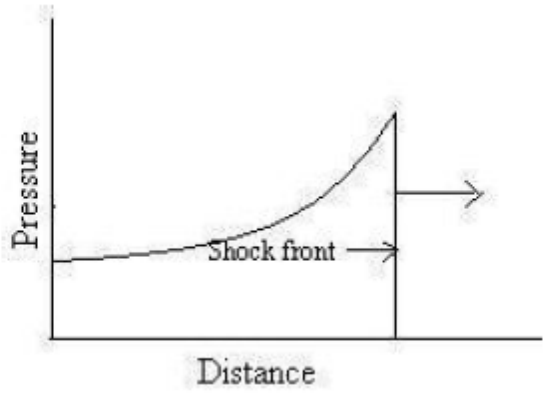


Fig 1.1 (a) Variation of pressure with distance

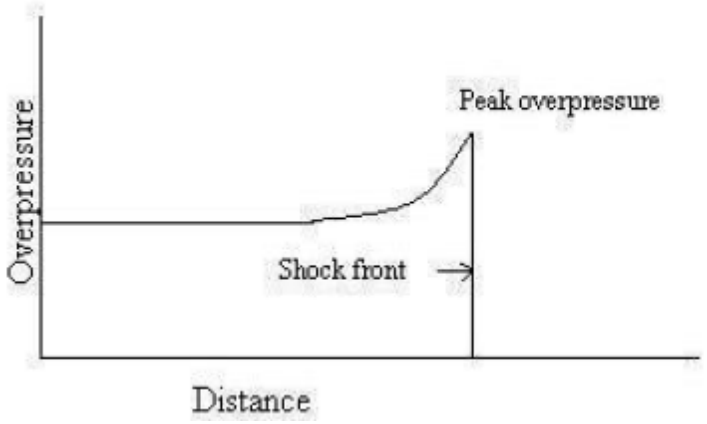


Fig.1.1 (b) Formation of shock front in a shock wave.

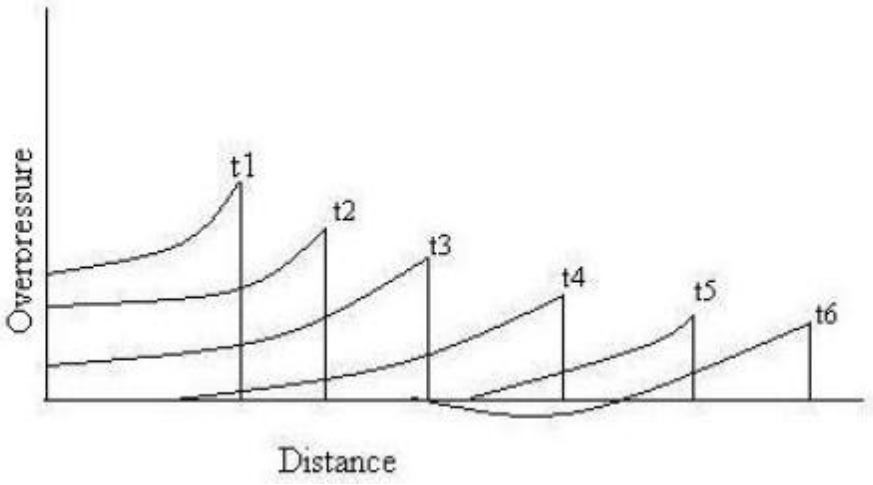


Fig.1.1 (c) Variation of overpressure with distance from centre of explosion at various times.

Mathematically the dynamic pressure Pd is expressed as:

$Pd=1/2\ \rho\ u2$

Where u is the velocity of the air particle and ρ is the air density

The peak dynamic pressure decreases with increasing distance from the centre of explosion, but the rate of decrease is different from that of the peak overpressure. At a given distance from the explosion, the time variation of the dynamic Pd behind the shock front is somewhat similar to that of the overpressure Ps, but the rate of decrease is usually different. For design purposes, the negative phase of the overpressure in Fig.1.2 (b) is not important and can be ignored.

Explosive and impact loads similar to and different from loads typically used in building design. Explosive loads and impact loads are transients, or loads that are applied dynamically as one-half cycle of high amplitude, short duration air blast or contact and energy transfer related pulse. This transient load is applied only for a specific and typically short period of time in the case of blast loads, typically less than one-tenth of a second. This means that an additional set of dynamic structural properties not typically considered by the designer, such as rate dependant material properties and inertial effects must be considered in design.

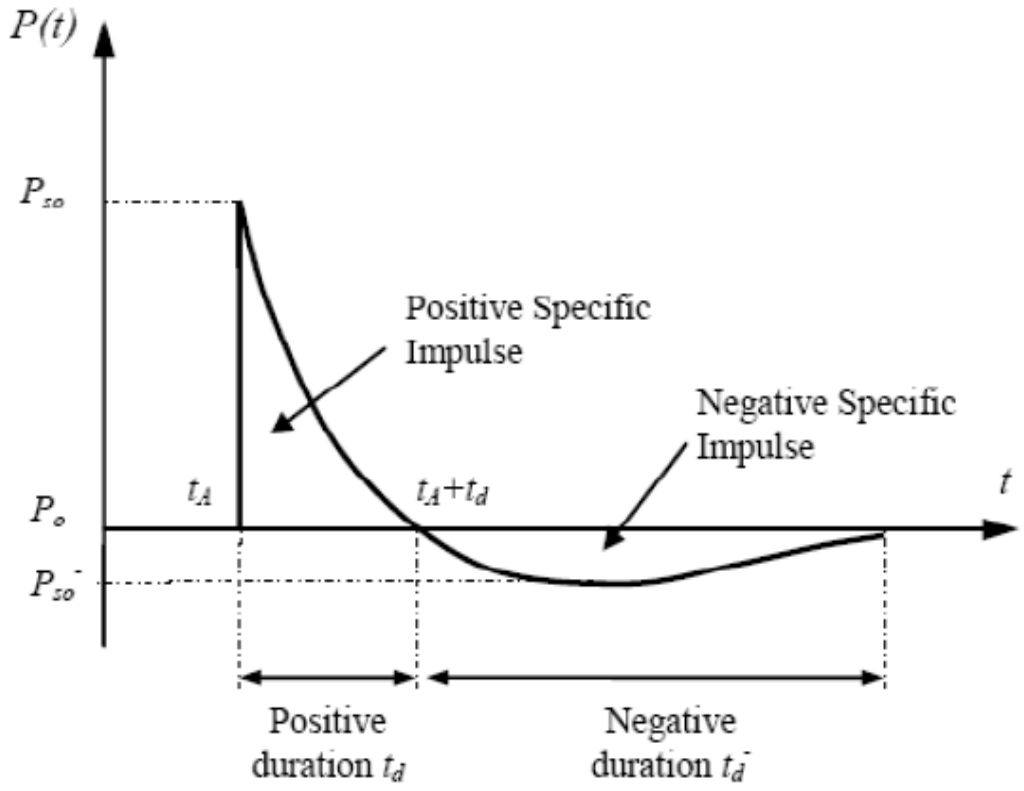


Fig.1.2 (a) The variation of overpressure with distance at a given time from centre of explosion.

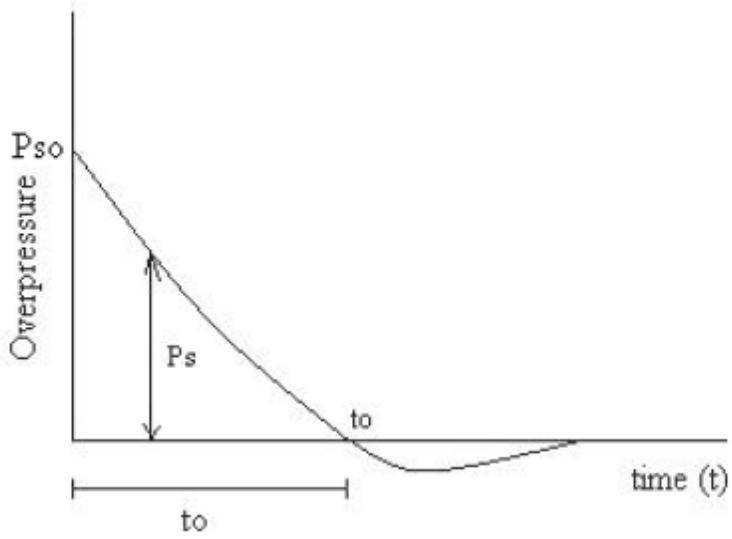


Fig.1.2 (b) Variation of overpressure with distance at a time from the explosion.

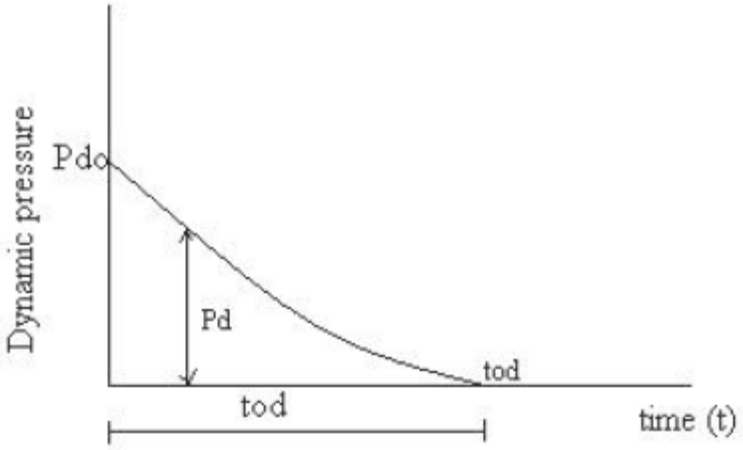


Fig.1.2(c) Variation of dynamic pressure with distance at a time from the explosion.

Often, design to resist blast, impact and other extraordinary loads must be thought of in the context of life safety, not in terms of serviceability or life-cycle performance. Performance criteria for other critical facilities (nuclear reactors, explosive and impact test facilities, etc.) may require serviceability and reuse, but most commercial office and industrial facilities will not have to perform to these levels. Structures designed to resist the effects of explosions and impact are permitted to contribute all of their resistance, both material linear and non-linear (elastic and inelastic), to absorb damage locally, so as to not compromise the integrity of the entire structure.It is likely that local failure can and may be designed to occur, due to the uncertainty associated with the loads.

**How blast loads are different from seismic loads:**

Blast loads are applied over a significantly shorter period of time (orders-of-magnitude shorter) than seismic loads. Thus, material strain rate effects become critical and must be accounted for in predicting connection performance for short duration loadings such as blast.

Also, blast loads generally will be applied to a structure non-uniformly, i.e., there will be a variation of load amplitude across the face of the building, and dramatically reduced blast loads on the sides and rear of the building away from the blast. Figure 1.3 shows a general comparison between an acceleration record from a point 7 km from the 1994 Northridge epicenter and the predicted column loads for the 1995 Oklahoma City bombing.

It is apparent that the 12-second-long ground shaking from the Northridge event lasted approximately 1000 times longer than the 9 ms initial blast pulse from the Murrah Building blast. The effects of blast loads are generally local, leading to locally severe damage or failure. Conversely, seismic "loads" are ground motions applied uniformly across the base or foundation of a structure. All components in the structure are subjected to the "shaking" associated with this motion.

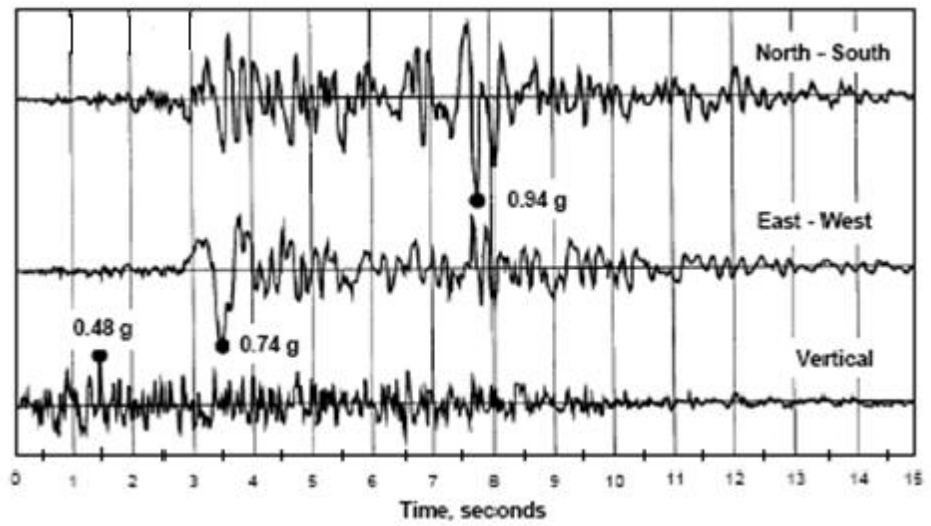


(a) Response of seismic loading on structure.

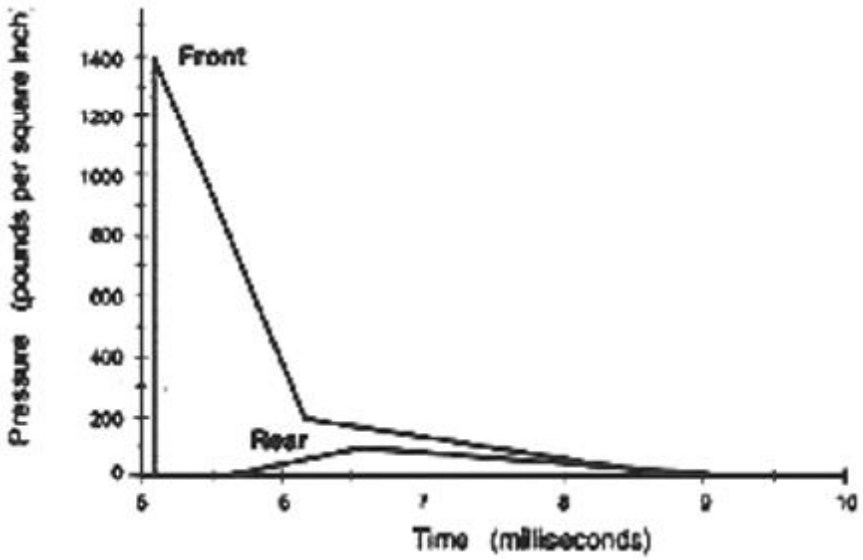


(b) Response of blast loading on structure.

Fig.1.3. Comparison between seismic load and the blast load

# CHAPTER 2

# BEHAVIOUR OF BUILDING UNDER BLAST LOADING

## 2.1 EXPLOSIVE AIR BLAST LOADING

The threat for a conventional bomb is defined by two equally important elements, the bomb size, or charge weight W, and the standoff distance (R) between the blast source and the target (Fig.2.1). For example, the blast occurred at the basement of World Trade Centre in 1993 has the charge weight of 816.5 kg TNT. The Oklahoma bomb in 1995 has a charge weight of 1814 kg at a standoff of 5m. As terrorist attacks may range from the small letter bomb to the gigantic truck bomb as experienced in Oklahoma City, the mechanics of a conventional explosion and their effects on a target must be addressed.

Throughout the pressure-time profile, two main phases can be observed; portion above ambient is called positive phase of duration (td), while that below ambient is called negative phase of duration (td). The negative phase is of a longer duration and a lower intensity than the positive duration. As the stand-off distance increases, the duration of the positive-phase blast wave increases resulting in a lower-amplitude, longer-duration shock pulse. Charges situated extremely close to a target structure impose a highly impulsive, high intensity pressure load over a localized region of the structure; charges situated further away produce a lower-intensity, longer-duration uniform pressure distribution over the entire structure. Eventually, the entire structure is engulfed in the shock wave, with reflection and diffraction effects creating focusing and shadow zones in a complex pattern around the structure. During the negative phase, the weakened structure may be subjected to impact by debris that may cause additional damage. STAND-OFF DISTANCE

Stand-off distance refers to the direct, unobstructed distance between a weapon and its target.

HEIGHT OF BURST (HOB)

Height of burst refers to aerial attacks. It is the direct distance between the exploding weapon in the air and the target.

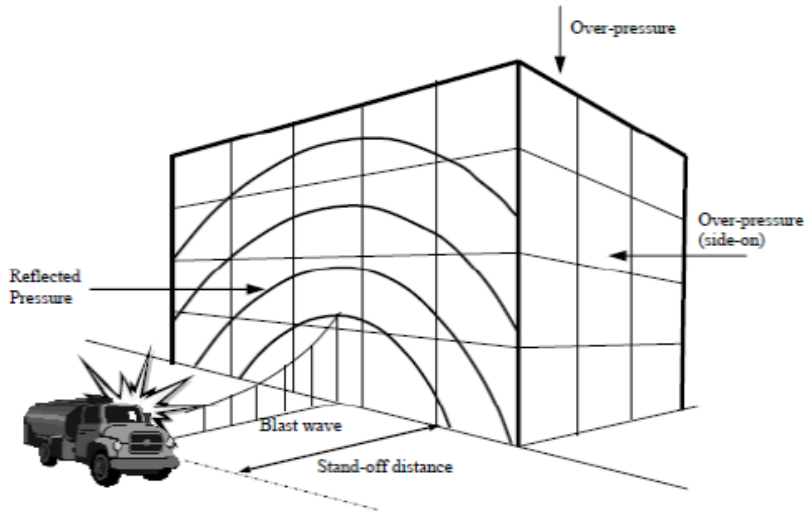


**Figure 2.1: Blast Loads on a Building**

If the exterior building walls are capable of resisting the blast load, the shock front penetrates through window and door openings, subjecting the floors, ceilings, walls, contents, and people to sudden pressures and fragments from shattered windows, doors, etc. Building components not capable of resisting the blast wave will fracture and be further fragmented and moved by the dynamic pressure that immediately follows the shock front. Building contents and people will be displaced and tumbled in the direction of blast wave propagation. In this manner the blast will propagate through the building.

## 2.2 BLAST WAVE SCALING LAWS

All blast parameters are primarily dependent on the amount of energy released by a detonation in the form of a blast wave and the distance from the explosion. A universal normalized description of the blast effects can be given by scaling distance relative to (E/Po)1/3 and scaling pressure relative to Po,

where E is the energy release (kJ) and Po the ambient pressure (typically 100 kN/m2).

For convenience, however, it is general practice to express the basic explosive input or charge weight W as an equivalent mass of TNT. Results are then given as a function of the dimensional distance parameter,

$$\text{Scaled Distance}\,(Z) = \frac{R}{W^{1/3}}$$

Where R is the actual effective distance from the explosion.

W is generally expressed in kilograms.

Scaling laws provide parametric correlations between a particular explosion and a standard charge of the same substance.

**2.3 PREDICTION OF BLAST PRESSURE**

Blast wave parameter for conventional high explosive materials have been the focus of a number of studies during the 1950's and 1960's.

The estimations of peak overpressure due to spherical blast based on scaled distance

Z=R/W (1/3) was introduced by Brode (1955) as:

$$P_{so} = \frac{6.7}{Z^3} + 1 \text{ bar} \quad (P_{so} > 10\text{bar})$$

$$P_{so} = \frac{0.975}{Z} + \frac{1.455}{Z^2} + \frac{5.85}{Z^3} - 0.019 \text{ bar} \quad (0.1 < P_{so} < 10 \text{ bar})$$

In 1961, Newmark and Hansen introduced a relationship to calculate the maximum blast pressure

(Pso), in bars, for a high explosive charge detonates at the ground surface as:

$$Pso = 6784 \frac{W}{R^3} + 93\left(\frac{W}{R^3}\right)^{1/2}$$

In 1987, Mills introduces another expression of the peak overpressure in kpa, in which W is the equivalent charge weight in kilograms of TNT and Z is the scaled distance.

$$P_{so} = \frac{1772}{Z^3} - \frac{114}{Z^2} + \frac{108}{Z}$$

As the blast wave propagates through the atmosphere, the air behind the shock front is moving outward at lower velocity. The velocity of the air particles, and hence the wind pressure, depends on the peak overpressure of the blast wave. This later velocity of the air is associated with the dynamic pressure, q(t). The maximum value, q(s), say, is given by

$$q(s) = 5\, P_{so}2/2\, (P_{so}+7\, P_o)$$

If the blast wave encounters an obstacle perpendicular to the direction of propagation, reflection increase the overpressure to a maximum reflected pressure Pr as:

$$P_r = 2\ P_{so}\ \{\frac{7\ P_o + 4\ P_{so}}{7\ P_o + P_{so}}\}$$

A full discussion and extensive charts for predicting blast pressures and blast durations are given by Mays and Smith (1995) and TM5-1300 (1990). Some representative numerical values of peak reflected overpressure are given in Table 1

Table 1. Peak reflected overpressures *Pr* (in MPa) with different W-R combinations

| W / R | **100 kg TNT** | **500 kg TNT** | **1000 kg TNT** | **2000 kg TNT** |
|---|---|---|---|---|
| 1m | 165.8 | 354.5 | 464.5 | 602.9 |
| 2.5m | 34.2 | 89.4 | 130.8 | 188.4 |
| 5m | 6.65 | 24.8 | 39.5 | 60.19 |
| 10m | 0.85 | 4.25 | 8.15 | 14.7 |
| 15m | 0.27 | 1.25 | 2.53 | 5.01 |
| 20m | 0.14 | 0.54 | 1.06 | 2.13 |
| 25m | 0.09 | 0.29 | 0.55 | 1.08 |
| 30m | 0.06 | 0.19 | 0.33 | 0.63 |

For design purposes, reflected overpressure can be idealized by an equivalent triangular pulse of maximum peak pressure Pr and time duration td, which yields the reflected impulse (ir).

$$\text{Reflected Impulse } (i_r) = \frac{1}{2} P_r t_d$$

Duration td is related directly to the time taken for the overpressure to be dissipated. Overpressure arising from wave reflection dissipates as the perturbation propagates to the edges of the obstacle at a velocity related to the speed of sound (Us) in the compressed and heated air behind the wave front. Denoting the maximum distance from an edge as S (for example, the lesser of the height or half the width of a conventional building), the additional pressure due to reflection is considered to reduce from Pr – Pso to zero in time 3S/Us. Conservatively, Us can be taken as the normal speed of sound, which is about 340 m/s, and the additional impulse to the structure evaluated on the assumption of a linear decay. After the blast wave has passed the rear corner of a prismatic obstacle, the pressure similarly propagates on to the rear face; linear build-up over duration 5S/Us has been suggested.

For skeletal structures the effective duration of the net overpressure load is thus small, and the drag loading based on the dynamic pressure is then likely to be dominant. Conventional

wind loading pressure coefficients may be used, with the conservative assumption of instantaneous build-up when the wave passes the plane of the relevant face of the building, the loads on the front and rear faces being numerically cumulative for the overall load effect on the structure.

Various formulations have been put forward for the rate of decay of the dynamic pressure loading; a parabolic decay (i.e. corresponding to a linear decay of equivalent wind velocity) over a time equal to the total duration of positive overpressure is a practical approximation.

## 2.4 STRUCTURAL RESPONSE TO BLAST LOADING

Complexity in analyzing the dynamic response of blast-loaded structures involves the effect of high strain rates, the non-linear inelastic material behavior, the uncertainties of blast load calculations and the time-dependent deformations. Therefore, to simplify the analysis, a number of assumptions related to the response of structures and the loads has been proposed and widely accepted. To establish the principles of this analysis, the structure is idealized as a single degree of freedom (SDOF) system and the link between the positive duration of the blast load and the natural period of vibration of the structure is established. This leads to blast load idealization and simplifies the classification of the blast loading regimes.

## 2.5 ELASTIC SDOF SYSTEMS

The simplest discretization of transient problems is by means of the SDOF approach. The actual structure can be replaced by an equivalent system of one concentrated mass and one weightless spring representing the resistance of the structure against deformation. Such an idealized system is illustrated in Fig.2.2. The structural mass, M, is under the effect of an external force, F(t), and the structural resistance, Rm, is expressed in terms of the vertical displacement, y, and the spring constant, K.

The blast load can also be idealized as a triangular pulse having a peak force Fm and positive phase duration td (see Figure 2.2). The forcing function is given as

$$F(t) = F_m\left(1 - \frac{t}{t_d}\right)\ldots$$

The blast impulse is approximated as the area under the force-time curve, and is given by

$$I = \frac{1}{2}F_m t_d$$

The equation of motion of the un-damped elastic SDOF system for a time ranging from 0 to the

positive phase duration, *td*, is given by Biggs (1964) as

$$M\ddot{y} + Ky = F_m\left(1 - \frac{t}{t_d}\right).$$

The general solution can be expressed as:

$$\text{Displacement } y(t) = \frac{F_m}{K}(1 - \cos\omega t) + \frac{F_m}{Kt_d}\left(\frac{\sin\omega t}{\omega} - t\right).$$

$$\text{Velocity } \dot{y}(t) = \frac{dy}{dt} = \frac{F_m}{K}\left[\omega\sin\omega t + \frac{1}{t_d}(\cos\omega t - 1)\right] \ldots$$

in which ω is the natural circular frequency of vibration of the structure and T is the natural

period of vibration of the structure which is given by

$$\omega = \frac{2\pi}{T} = \sqrt{\frac{K}{M}} \ldots$$

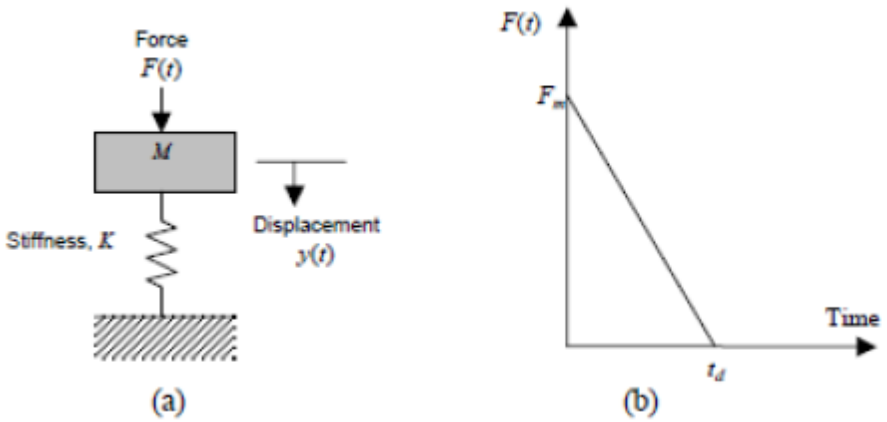


Figure 2.2 (a) SDOF system and (b) blast loading

The dynamic load factor, DLF, is defined as the ratio of the maximum dynamic deflection ym to the static deflection yst which would have resulted from the static application of the peak load Fm, which is shown as follows:

$$DLF = \frac{Y_{max}}{Y_{st}} = \frac{Y_{max}}{F_m / K} = \psi(\omega t_d) = \psi\left(\frac{t_d}{T}\right)$$

The structural response to blast loading is significantly influenced by the ratio td/T or ωtd (td/T

= ωtd/ 2π ). Three loading regimes are categorized as follows:

- ωtd < 0.4 : impulse loading resime.

- ωtd < 0.4 : quasi-static resime.

- 0.4 < ωtd < 40 : dynamic loading resime.

**2.6 ELASTO-PLASTIC SDOF SYSTEMS**

Structural elements are expected to undergo large inelastic deformation under blast load or high velocity impact. Exact analysis of dynamic response is then only possible by step-by-step numerical solution requiring nonlinear dynamic finite- element software. However, the degree of uncertainty in both the determination of the loading and the interpretation of acceptability of the resulting deformation is such that solution of a postulated equivalent ideal elasto-plastic SDOF system (Biggs, 1964) is commonly used. Interpretation is based on the required ductility factor μ = ym/ye. For example, uniform simply supported beam has first mode shape φ(x) = sin πx/L and the equivalent mass M = (1/2)mL, where L is the span of the beam and m is mass per unit length.

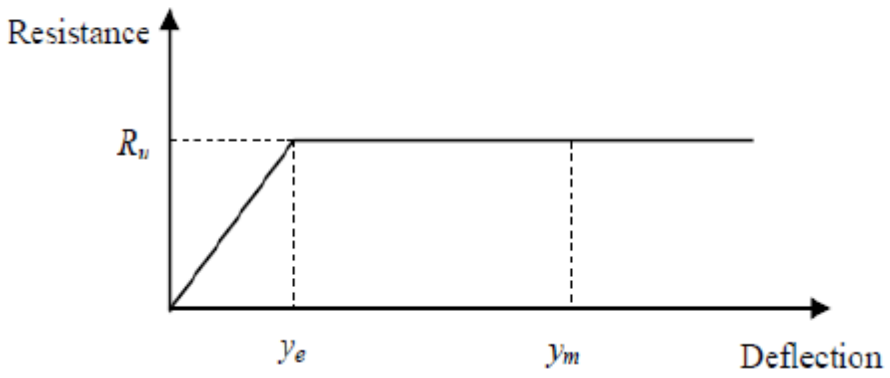


Figure 2.3 Simplified resistance function of an elasto-plastic SDOF system

The equivalent force corresponding to a uniformly distributed load of intensity p is F = (2/π)pL. The response of the ideal bilinear elasto-plastic system can be evaluated in closed form for the triangular load pulse comprising rapid rise and linear decay, with maximum

value Fm and duration td. The result for the maximum displacement is generally presented in chart form TM 5- 1300, as a family of curves for selected values of Ru/Fm showing the required ductility μ as a function of td/T, in which Ru is the structural resistance of the beam and T is the natural period (Figure 2.4).

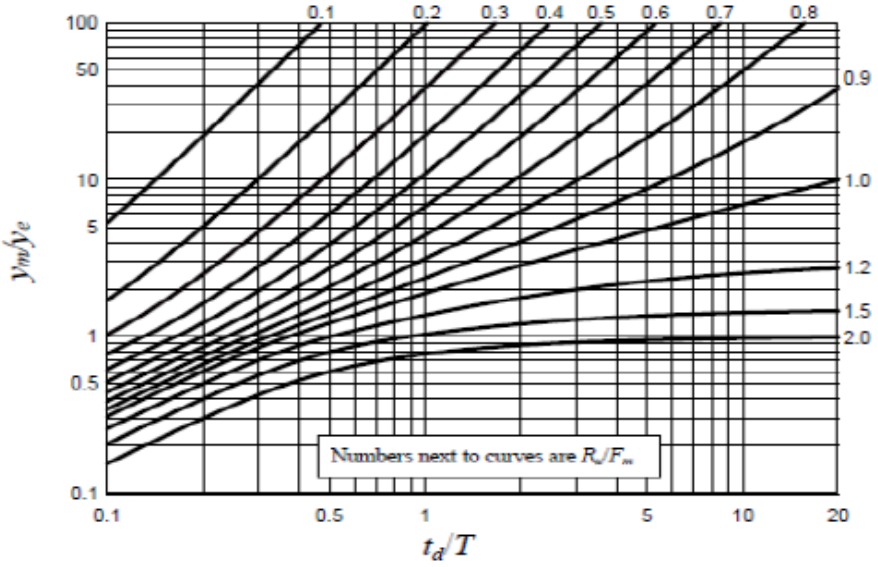


Figure 2.4 Maximum response of elasto-plastic SDF system to a triangular load.

## 2.7 MATERIAL BEHAVIORS AT HIGH STRAIN RATE

Blast loads typically produce very high strain rates in the range of $10^2 – 10^4$ $S^{-1}$. This high loading rate would alter the dynamic mechanical properties of target structures and, accordingly,the expected damage mechanisms for various structural elements. For reinforced concrete structures subjected to blast effects the strength of concrete and steel reinforcing bars can increase significantly due to strain rate effects. Figure 2.5 shows the approximate ranges of the expected strain rates for different loading conditions. It can be seen that ordinary static strain rate is located in the range: $10^{-6}$-$10^{-5}$ $S^{-1}$ ,while blast pressures normally yield loads associated with strain rates in the range: $10^2 – 10^4$ $S^{-1}$

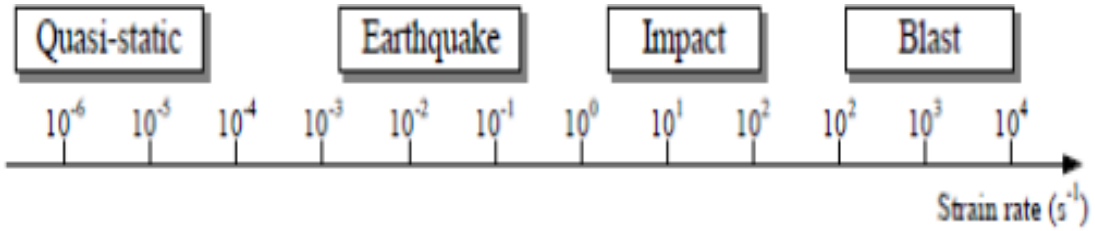


Figure 2.5 Strain rates associated with different types of loading.

## 2.8 DYNAMIC PROPERTIES OF CONCRETE UNDER HIGH- STRAIN RATES

The mechanical properties of concrete under dynamic loading conditions can be quite different from that under static loading. While the dynamic stiffness does not vary a great deal from the static stiffness, the stresses that are sustained for a certain period of time under dynamic conditions may gain values that are remarkably higher than the static compressive strength (Figure 2.6). Strength magnification factors as high as 4 in compression and up to 6 in tension for strain rates in the range: $10^2$–$10^3$ /sec have been reported (Grote et al., 2001).

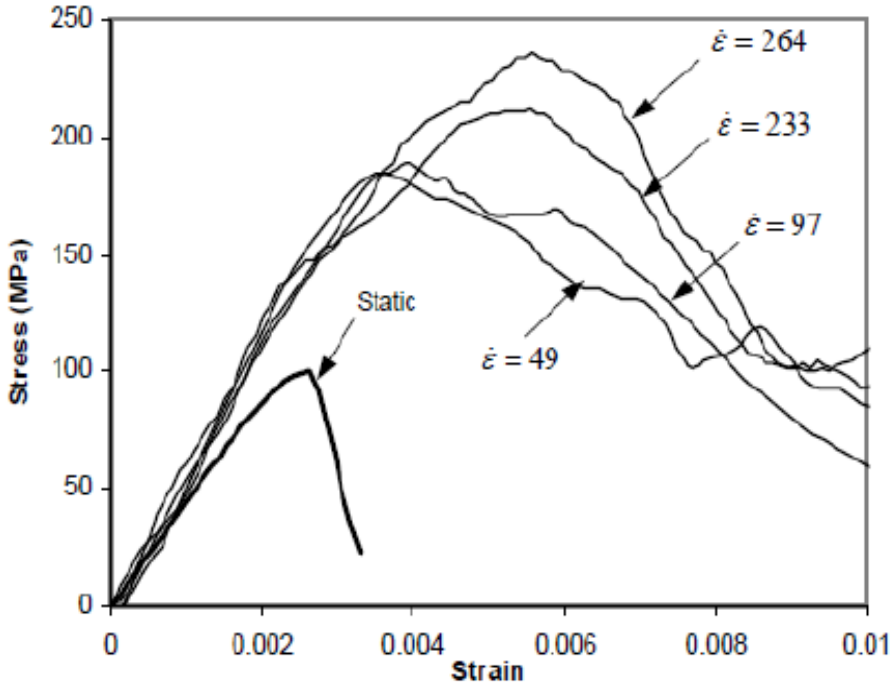


Figure 2.6 Stress-strain curves of concrete at different strain rates.

For the increase in peak compressive stress (f'c), a dynamic increase factor (DIF) is introduced in the CEB-FIP (1990) model (Figure 3.10) for strain-rate enhancement of concrete as follows:

$$DIF = \left\{ \frac{\dot{\varepsilon}}{\dot{\varepsilon}_s} \right\}^{1.026\alpha} \quad \text{for} \quad \dot{\varepsilon} \le 30s^{-1}.$$

$$DIF = \gamma \left\{ \frac{\dot{\varepsilon}}{\dot{\varepsilon}_S} \right\}^{1/3} \quad \text{for} \quad \dot{\varepsilon} \le 30s^{-1}$$

where:

$\dot{\varepsilon}$ = strain rate ,

$\dot{\varepsilon}_s = 30\times10^{-6}s^{-1}$ (quasi-static strain rate)

$\log y = 6.156\ \alpha - 2$

$\alpha = 1/(5 + 9\ f'c/fco)$

$fco$ = 10 MPa = 1450 psi

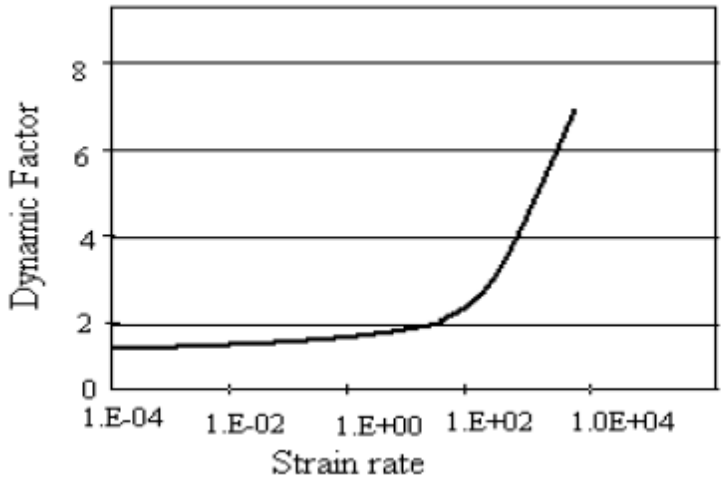


Figure 2.7 Dynamic Increase Factor (DIF) for peak stress of concrete.

## 2.9 DYNAMIC PROPERTIES OF REINFORCING STEEL UNDER HIGH-STRAIN RATES

Due to the isotropic properties of metallic materials, their elastic and inelastic response to dynamic loading can easily be monitored and assessed. Norris et al. (1959) tested steel with two different static yield strength of 330 Mpa and 278 MPa under tension at strain rates ranging from 10-5 to 0.1 S-1. Strength increase of 9 - 21% and 10 - 23 % were observed for the two steel types, respectively. Dowling and Harding (1967) conducted tensile experiments using the tensile version of Split Hopkinton's Pressure Bar (SHPB) on mild steel using strain rates varying between 10-3 S-1and 2000 S-1. It was concluded from this test series that materials of bodycentered cubic (BCC) structure (such as mild steel) showed the greatest strain rate sensitivity. It has been found that the lower yield strength of mild steel can almost be doubled; the ultimate tensile strength can be increased by about 50%; and the upper yield strength can be considerably higher. In contrast, the ultimate tensile strain decreases with

increasing strain rate. Malvar (1998) also studied strength enhancement of steel reinforcing bars under the effect of high strain rates

This was described in terms of the dynamic increase factor (DIF), which can be evaluated for different steel grades and for yield stresses, fy, ranging from 290 to 710 MPa as represented by equation

$$DIF = \left( \frac{\dot{\varepsilon}}{10^{-4}} \right)^{\alpha}$$

Where for calculating yield stress

$$\alpha = \alpha_{fy}$$

$$\alpha_{fy} = 0.074 - 0.04(f_y/414).$$

For ultimate stress calculation

$$\alpha = \alpha_{fy}$$

$$\alpha_{fy} = 0.019 - 0.009(f_y/414)$$

# CHAPTER 3

# MODELLING OF BUILDING

**3.1 B.M. Luccioni et al** studied the behaviour of structural elements and materials under blast loads. The experimental results about the behaviour of steel, concrete and fibre reinforced panels subjected to explosions were studied. Most of the results related to full-scale structures are those concerning structure

that have actually suffered explosions.

Many models were included in different computer programs, which can be used for the analysis of the blast behaviour of structural elements and small structures and validated with available experimental results. These were related to the effect of blast loads in reinforced concrete buildings and presents the results of the numerical simulation of the structural collapse of an actual building. The location and magnitude of the explosive load were previously obtained from the blast analysis and comparison with actual damage of the complete block of buildings where the target was located and are supposed to be known in this paper. It is assumed that the damage was caused by an explosive load equivalent to 400 kg of TNT placed in the entrance hall of the building.

### 3.1.1 Computation model

The computational model was constructed as per the structural and architectural plans of the actual building. For the dynamical analysis of building structures under seismic or wind loads, it was enough to model only the resisting structure. A blast analysis also required the consideration of all the non-structural elements, specially the walls as they play an important role in the propagation of the pressure wave.

***Parts of the model***

The model was composed of the building and air volume occupied by the building.

A 3D Euler FCT [9](higher order Euler processor) subgrid was used for the air. The lateral faces of the underground level were supposed to have rigid surfaces and air flow out was allowed in the rest of the borders.

The complete building was modelled, from the underground level to the higher level. The resulting model is presented in Fig. 3.1. As it can be seen in this figure, the building was composed of three differentiable blocks: the front block, severely damaged by the blast load,

the intermediate block and the back block. The mesh was refined and a more detailed modelling was used in the front block were the focus of the explosion was expected.

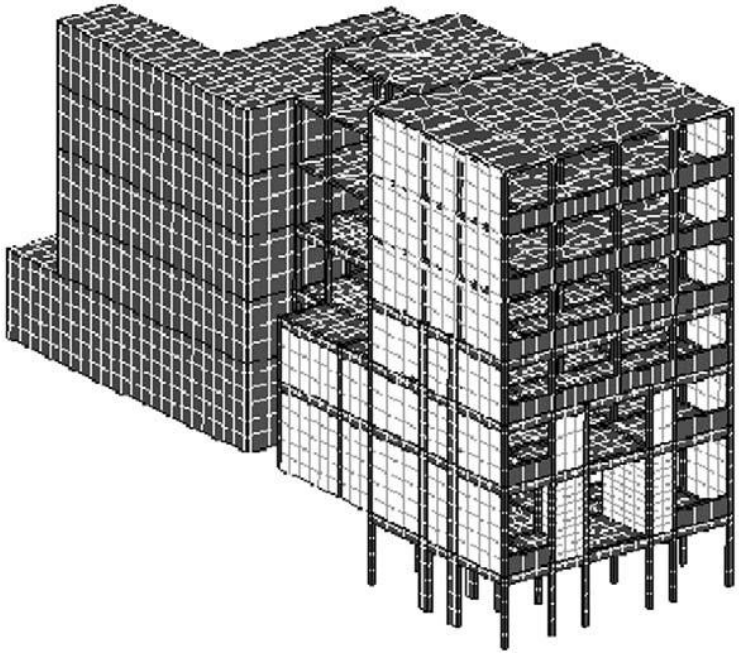

Fig. 3.1 Model for the complete building

The model of the building was composed of the reinforced concrete structure and the masonry walls. A rigid floor in the bottom of the underground level was used to simulate the soil. The reinforced concrete structure was a frame structure composed by columns, beams and slabs. The mesh was finer in the front of the building and the lower levels. A coarse discretization was used for the back part of the building, not affected by the explosion and with no significance in the structural collapse.

The columns, beams and slabs were modelled with 3D solid elements that were solved with a Lagrange processor. The base of the columns were fixed in their base corresponding to the ground level in the back part of the building and the underground level in the front. The exterior and interior walls of the first level, where the explosion was supposed to have taken place, were modelled with shell elements of 30 cm of thickness and solved with a Lagrange processor. As the walls in the building were in filled masonry walls, they were modeled as perfectly joined to the reinforced concrete frame. The loads were transferred to the frames through the common nodes.

**Analysis:**

The analysis of the structural collapse of the building was performed in two stages. The first part of the analysis consists on the simulation of the explosion itself from the detonation instant and the second part consists on the analysis of the effect and interaction with the building of the blast wave generated by the explosion. Only the load produced by the air blast wave was considered in the analysis. The ground motion generated by the explosion was not taken into account because the explosive was supposed to be placed 1 m above the ground level, for example on a vehicle, isolated from the ground and so the ground shock can be diminished .


**Fig. 3.2.** Mesh used for the generation of the explosion (400 kg TNT)

The initiation of the explosion and the propagation of the blast wave in the air in contact with the explosive were first simulated. For this purpose, it was assumed that, until the blast wave encounters a rigid surface, the problem has spherical symmetry and can be treated as 1D. The results of this analysis were later mapped in the 3D model representing the building and the surrounded air volume.

The initial detonation and expansion of the sphere of 400 kg of TNT was modeled in a 1D, spherically symmetric model of 1 m radius with a JWL equation of state, as illustrated in Fig.3.2 Part way through the detonation process, and to avoid numerical errors, the material model for the high explosive was modified. The 1D expansion analysis continues until just prior to impingement of the blast wave on the rigid surface.

The TNT and air material data are shown in Table 2. The default density gave a radius 388.4 mm for a 400 kg spherical charge of TNT. Fig. 3.3 shows the remapping of the 1D analysis to the 3D model of the building.

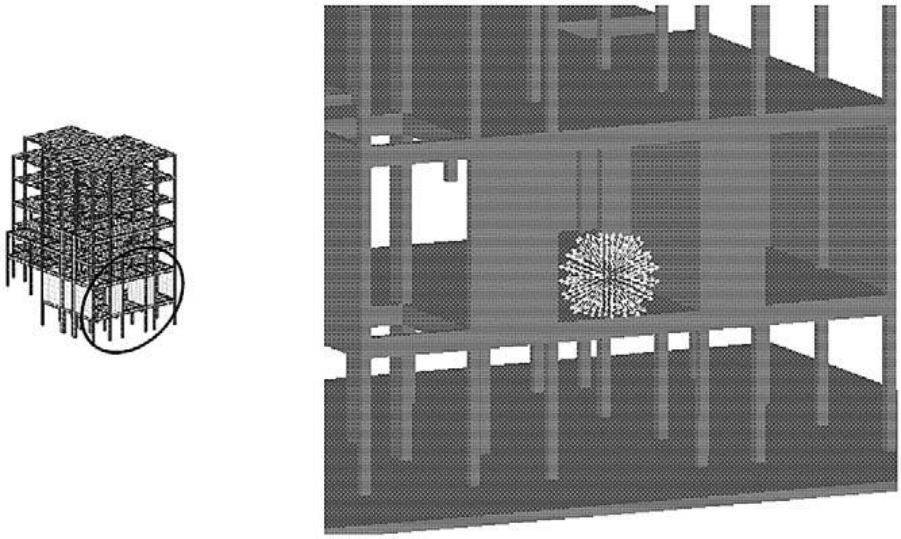

Fig. 3.3 Remapping to the 3D model (0.2 ms)

Table 2 Material properties for the explosion generation

| Material | Air | TNT | TNT (idal) |
|---|---|---|---|
| Equation of state | Ideal gas<br>$\gamma = 1.$<br>$\rho = 1.225$ x 10-3 g/cm$^3$<br>Ref. energy – 0.0 mJ<br>Press. Shift = 0.0 kPa | JWL<br>Standard<br>Library data | Ideal gas<br>$\gamma = 1.35$<br>$\rho = 1.0 \times 10^{-4}$ g/cm$^3$<br>Ref. energy – 0.0 mJ<br>Press. Shift = 0.0 kPa<br>From detonation model/remap datas |

The propagation of the blast wave and its interaction with the building was analysed. For that purpose, an interaction algorithm between the Lagrange (building) and Euler (air) processors was used.

Role played by the interaction of the blast wave with the building, the propagation of the blast wave in a building without walls was compared with the propagation of the same blast wave in the actual building with walls in Fig. 3.4. The velocity field was represented in the air and pressure contours were plotted on the solids. Due to reflections on the walls, the blast wave lost its spherical shape and increased its destructive effect in vertical direction.

In the analysis of the building collapse, the solid–solid interaction between the different parts of the structures that fell down was also taken into account.

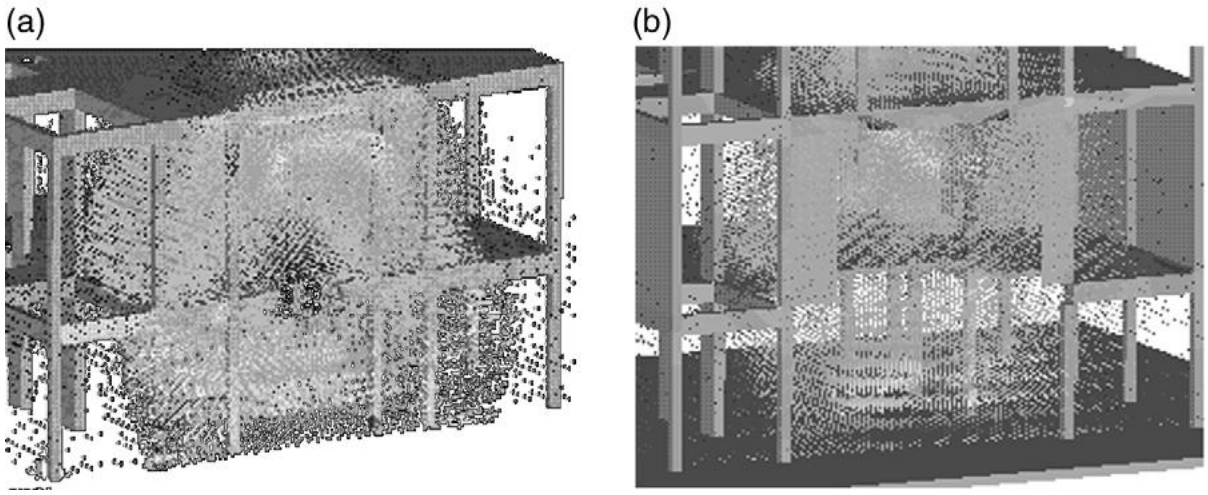


**Figure 3.4.** Effect of the wall in the blast wave propagation (a) Building without walls, (b) building with walls.

**Effects:**

The results obtained for an explosive load of 400 kg of TNT located 1 m above the ground level, 1 m inside the entrance hall and 1 m to the right of the axis of the building are shown in Fig. 3.5. For the sake of visualization, only the front and the intermediate blocks of the building are shown. The first moments following the detonation are shown in Fig. 3.5a. The erosion of most of the columns and walls in the first stage and the underground stage, in the front block, is showed in Fig. 3.5b. The failure of the highest slab and the loosening of the front block are clear in Fig. 3.5c. The free fall of the front block can be seen in Fig. 3.5d. The final state of the collapsed structure can be observed in Fig. 3.5e.

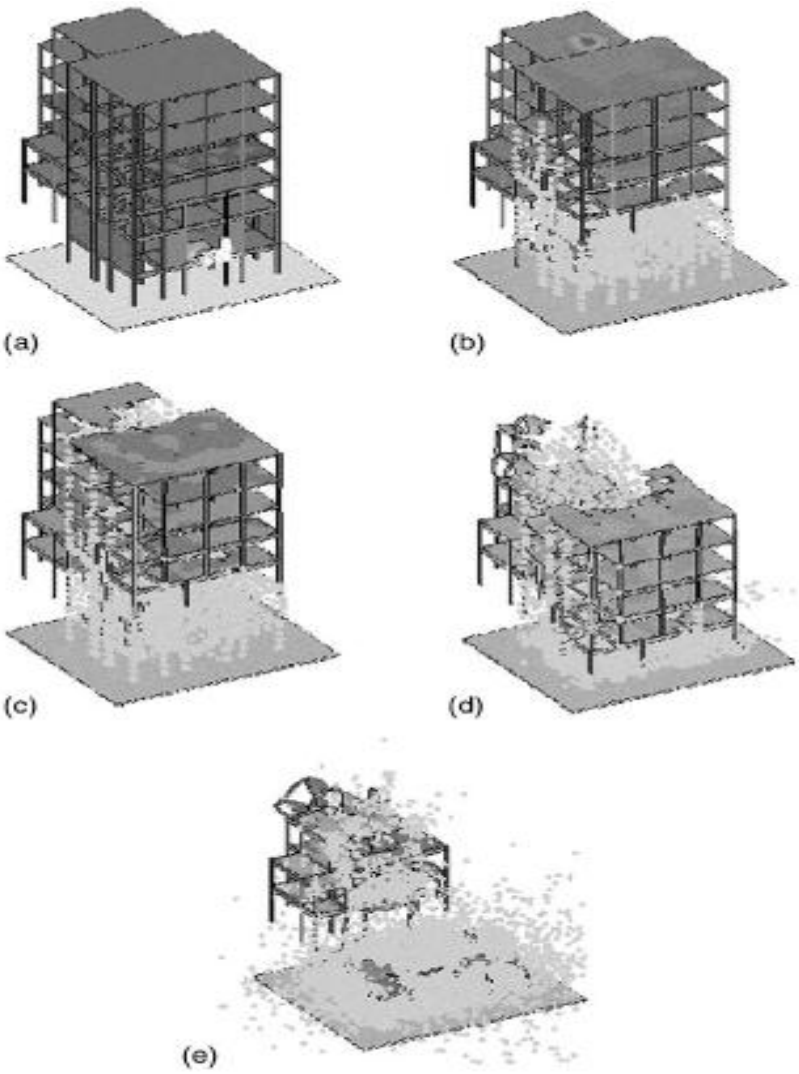


Fig. 7. Evolution of damage produced by the explosion. (a) 0.75 ms, (b) 254 ms, (c) 378 ms, (d) 1.35 ms and (e) 2.46 ms.

*Collapse mechanism*

The structural collapse was due to a gravitational mechanism produced by the failure of most of the load bearing columns of the first stage in the front block.

The four columns closer to the explosion focus failed due to the direct effect of the reflected pressure that produced the erosion of concrete by brisance effect (see Fig. 3.5a). Lateral columns in the front failed by a combination of shear and flexure. Columns at the back of the front block lost connection with the upper and lower beams (tension failure), due to the tension effect imparted by the first floor slabs that were pushed upwards and downwards by the pressure and then failed by lack of lateral support when the pressure wave reached them.

The pressure destroyed the ground floor just under the explosion (see Fig. 3.5a) allowing the blast wave to pass to the underground level and destroy some columns (see Fig. 3.5b). The first three lines of columns of the underground level and the first level were almost completely destroyed (Fig. 3.5b) leaving without support the upper floors that began to fall down pulling from the back block (Fig. 3.5c). Beams and columns in the upper floors of the intermediate block have failed by a combination of tension, flexure and shear.

On the other side, the blast wave propagated upwards in the intermediate block, limiting the advance of damage to the back block. See Fig. 3.5b. Both effects produced an inclined failure advancing backwards in height. See Fig. 3.5e. The front block lost connection with the rest of the structure along this inclined line and immediately began to fall down. The slabs impacted one over the other destroying themselves.

**3.2 Chengqing Wu et al** has studied 3D homogenized model for masonry including equivalent elastic moduli, strength envelope and failure characteristics , and material damage model developed for reinforced concrete structures was employed to investigate the influences of simultaneous ground shock and airblast forces on structural responses. Simultaneous ground shock and airblast forces, which are estimated from a previous study are used as input for the analysis. The developed material models for masonry and RC were implemented into a finite element computer program LS-DYNA3D as its user defined subroutines. A single story masonry infilled RC frame was employed as an example structure. The response characteristics and collapse of the example structure to simultaneous ground shock and airblast forces, or separately to ground shock only or airblast forces only at different scaled distances are simulated and observed.

**Structural response and damage:**

The above numerical models for masonry and reinforced concrete are programmed and linked to LSDYNA as its user defined subroutines in the present study to simulate structural response. As the primary objective of the study is to investigate the relative importance of ground shock on structural response and damage to adjacent surface explosion, a one-story masonry infilled RC frame is employed in the analysis as an example structure. The configuration of the one-story masonry infilled RC frame is shown in Fig. 3.6. The span length and height of the structure are 5.0 and 3.3 m, respectively. The roof slab thickness is 150mm and floor width is 5m. The columns and beams have a cross section of 300*300mm and 200*300mm with a 2% reinforcement ratio. The grade of concrete is C30 with elastic modulus $E_c$ = 27 GPa and shear modulus $G_c$= 14 GPa. The reinforcement is Grade S460 with Young's modulus $E_{s1}$ = 21 GPa, plastic hardening modulus $E_{s2}$ = 21 GPa and shear

modulus $G_{s1}$ = 80 GPa. The threshold strains adopted to characterize the failure property of concrete is $\varepsilon_0^-$ = 0:0035, $\varepsilon_0^+$= 0.00035, and reinforcement $\varepsilon_u^s = 0.02$.

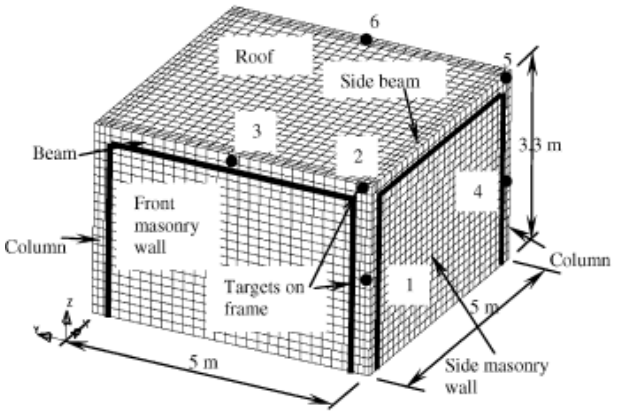


**Figure 3.6** Numerical model of one-story structure and targets on the structure

The thickness of the masonry wall is 240 mm. In the numerical model, the masonry walls are tied to the beams and columns on all sides using a tied failure contact slideline. These slidelines keep element faces together until a prescribed failure criterion is reached. The failure criterion is set to be equivalent to known data on the strength of mortar. Table 3 lists material properties for mortar. The imposed and dead load of 3 kN/m$^2$ on structural floors are also included in the analysis. Targets 1–6 on the structure are specified to record dynamic response on the mid height of the column, centers of the front and rear beams and the front and rear beam-column joints. The charge weight of TNT is assumed to be 1000 kg and the structural response to explosive loads at different scaled distances is simulated in the analysis. The influence of element size on computational accuracy is investigated before the numerical simulation. It is carried out by halving the size of the element for structural members until the difference between the results obtained with two consecutive element sizes is less than 5%. For example, the element size for column is 0.1m x 0.1m x 0.1 m.

Fig. 3.7 shows displacement distributions of the one-story building at 0.015 s after explosion at a scaled distance of 0.5 m/kg$^{1/3}$ obtained using, respectively, the simultaneous ground shock and airblast load, airblast load only, and ground shock only. As shown, under the cases of considering combined ground shock and airblast load, and

Table 3

| $E_c$ (GPa) | $G_c$(GPa) | $\nu$ | $\sigma_t$ (MPa) | $\sigma_c$ (MPa) |
|---|---|---|---|---|
| 5.8 | 2.2 | 0.33 | 1.0 | 14.0 |

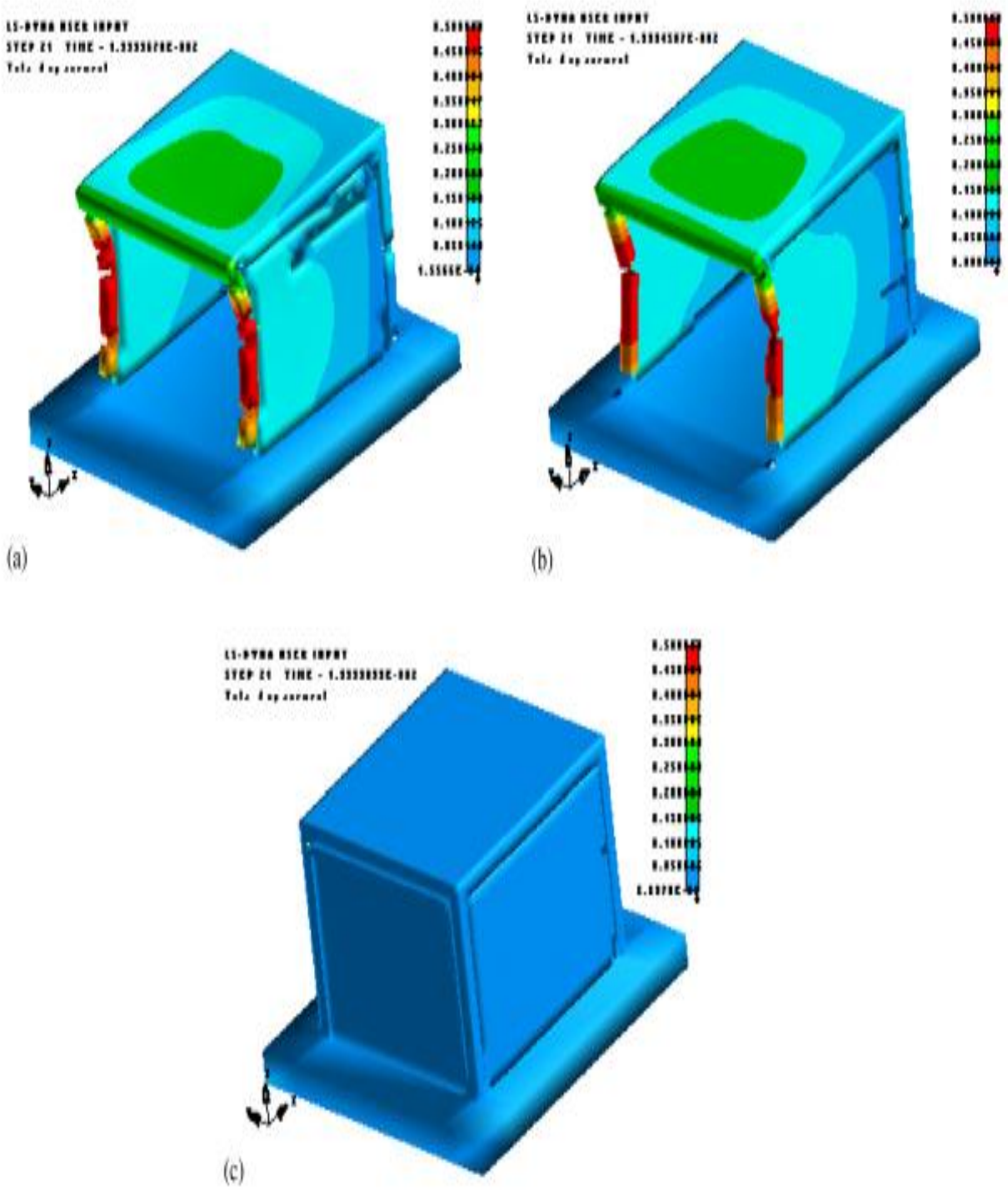


**Figure 3.7:** Displacement distribution of the structure at 0.015 s after explosion at scaled distance 0.5m/kg$^{1/3}$. (a) combined loads; (b) irblast loads; (c) ground shock.

Considering airblast load only, the front masonry wall and front columns were blown off immediately, and side walls, rear wall and rear columns suffer serious damage. The

contribution of ground shock on structural damage was prominent on front and rear columns and side walls. By comparing Fig. 3.7(a) and (b), it was obvious that including ground shock in the structural response analysis results in more severe damage in the front and rear columns and side walls of the structural model, although response and damage are governed primarily by airblast load. Collapses of the structure subjected to airblast load and combined load are observed from the simulation, but ground shock alone could not cause structure to collapse, as shown in Fig. 3.7 (c). These results demonstrate that when the structure is close to the explosion center, structural response and damage are governed by airblast load, and ground shock influence can be neglected, as most of codes and regulations do, although ground shock intensifies the structural response and damage. As the scaled distance increases, airblast load decreases rapidly. At a certain scaled distance, collapse of the structure under airblast load alone will not occur. Simulation shows that the critical scaled distance is 1.84 m/kg$^{1/3}$ (see Fig. 3.8b). However, when the structure is under combined ground shock and airblast load at this scaled distance, failure of front columns of the structure is observed and structure collapses (see Fig. 3.8a). These observations indicate that at this critical scaled distance, the ground shock influence cannot be neglected because neglecting it results in a critical under prediction of a collapsed structure as still standing.

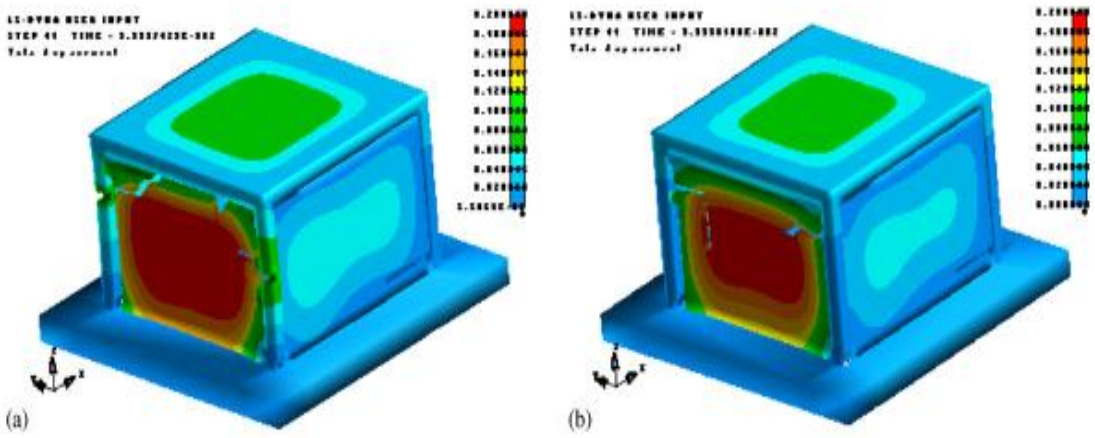


**Figure 3.8.** Displacement distribution of the structure at 0.05 s after explosion at scaled distance 1.84 m/kg$^{1/3}$. (a) combined loads; (b) airblast loads

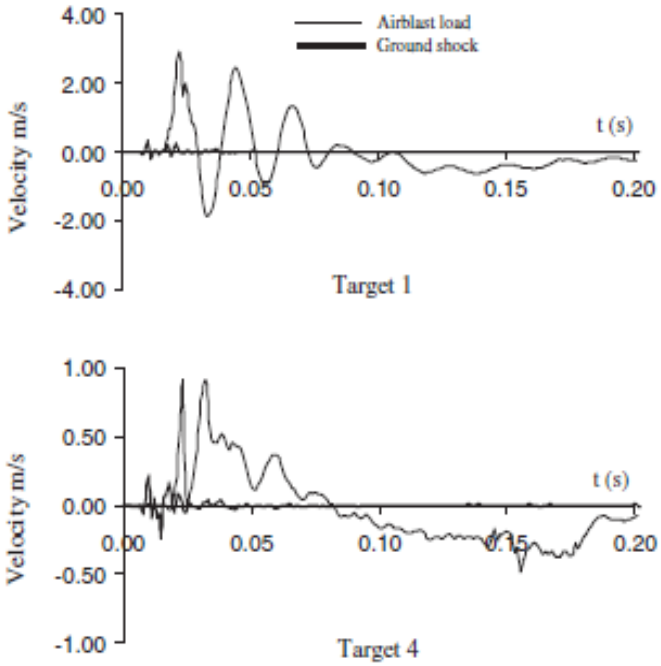


**Figure 3.9.** Velocity response time histories at target 1 and 4 obtained by ground shock and airblast force at scaled distance 1.84 m/kg$^{1/3}$.

Figure 3.9 shows peak velocity response value generated by ground a comparison of velocity response time histories at targets 1 and 4 obtained by ground shock alone and airblast force alone at the scaled distance of 1.84 m/kg1/3shock is only about one-tenth of that induced by airblast load at target 1 and one-fifth at target 4, but without considering ground shock, structure will not collapse under the airblast force alone at this critical distance. Fig. 3.10 shows a comparison of the velocity response time histories of the structure to combined load, ground shock only, and airblast forces only at targets 1–4 at scaled distance 3m/kg$^{1/3}$. As shown, the ground shock excites the structure first. After the arrival of the airblast force, although ground shock is no longer acting on the structure, the structure response is smaller if the ground shock is neglected. This is because the structure does not respond to airblast force from rest after the ground shock excitation. Nonetheless, airblast force results in larger structure response at targets 1, 2 and 3. At target 4, however, peak response generated by ground shock is comparable to that by airblast force.As compared with those shown in Fig. 3.9, the relative importance of ground shock effects on structures clearly increases, indicating that ground shock has significant influence on response at the middle height of the rear columns.

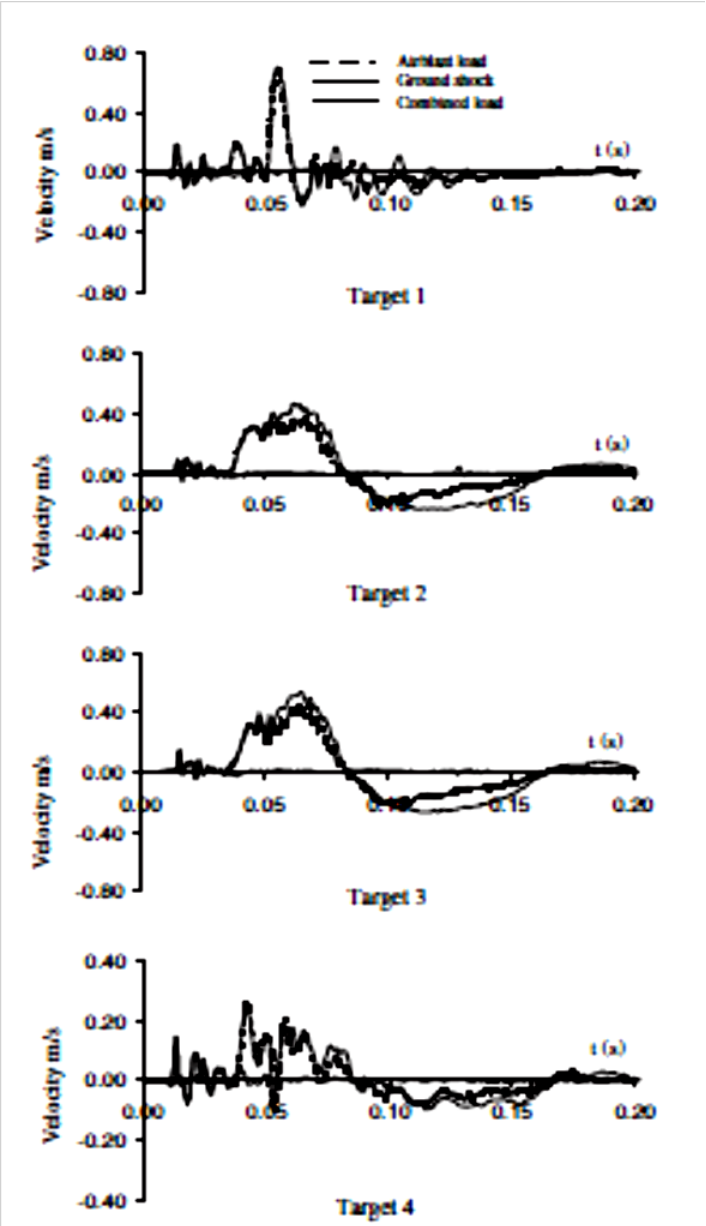


**Figure 3.10.** Velocity response time histories obtained by ground shock, airblast force and combined load at scaled distance 3 m/kg$^{1/3}$.

The simulation results, not shown here, also indicate that the front masonry wall subjected to airblast load and combined load collapses, but ground shock alone fails to cause the front masonry wall to collapse. These observations show that at distances immediately after the ground shock and airblast force coupling, airblast force still governs structural response and damage, but the effects of ground shock

increases. The corresponding displacement time histories at targets 1–4 at the scaled distance 3 m/kg$^{1/3}$ are illustrated in Fig. 3.11. It can be observed that the displacement time histories on targets 1–4 produced by combined load are obviously larger than those by airblast load alone. Thus including ground obviously larger than those by airblast load alone.

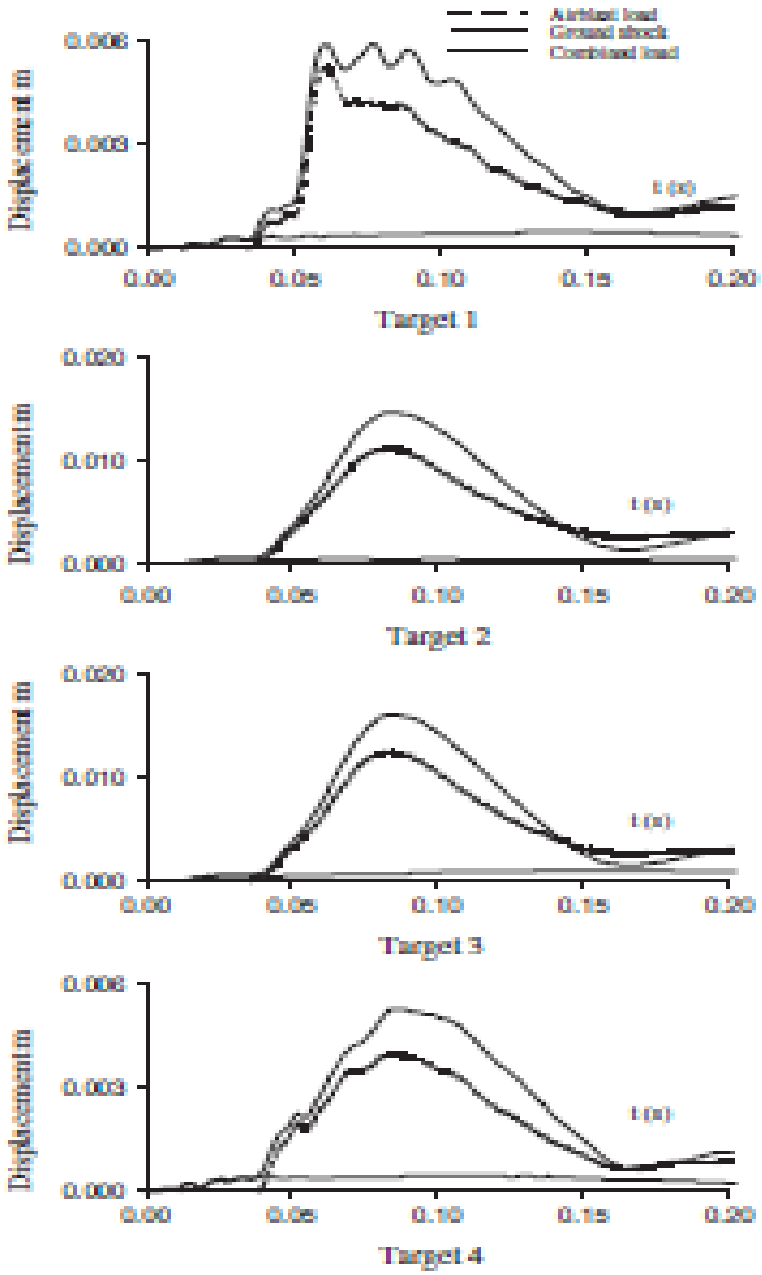


**Figure 3.11** Displacement response time histories obtained by ground shock, airblast force, and combined load at scaled distance 3 m/kg$^{1/3}$

# CHAPTER 4

# ESTIMATION OF BLAST LOAD

## *4.1 Estimation of blast load*

For calculating horizontal net pressure due to blast on a building, it is required to find the important parameter as follow

Scaled distance is computable by

$$Z = \frac{R}{W^{\frac{1}{3}}} \tag{4.1}$$

Where R is the distance from the centre of a spherical charge in meters and W is the charge mass expressed in kilograms of TNT.

Computation of pressures

The estimation of peak pressure due to blast based on scaled distance Z was introduced by Brode (1955)

$$P_s o = 6.7 / Z^3 + 1 bar \tag{4.2}$$

$P_{so}$>10bar

$$P_{so} = \frac{0.975}{Z} + \frac{1.455}{Z^2} + \frac{5.85}{Z^3} - 0.019 \text{ bar} \tag{4.3}$$

0.1<$P_{so}$<10bar

Newmark and Hansen introduced a relationship to calculate the maximum blast pressure (1961)

$$P_{so} = 6784 * \frac{W}{R^3} + 96 * (\frac{W}{R^3})^{\frac{1}{2}} \text{ bar} \tag{4.4}$$

Mills introduced another expression of the peak overpressure in KPa

$$P_{so} = \frac{1772}{Z^3} - \frac{114}{Z^2} + \frac{108}{Z} \tag{4.5}$$

As the blast wave propagates through the atmosphere, the air behind the shock front is moving outward at lower velocity. The velocity of the air particles, and hence the wind pressure, depends on the peak overpressure of the blast wave. This later velocity of the air is associated with the dynamic pressure, *q*(*t*). The maximum value, *q(s)*, say, is given by

$$q_{(s)} = \frac{5 * P_{so}^{\ 2}}{2 * (p_{so} + 7 * P_o)} \tag{4.6}$$

Or

$$q_{(s)} = \frac{P_{so}^{\ 2}}{(0.4 p_{so} + 41.2)} \tag{4.7}$$

If the blast wave encounters an obstacle perpendicular to the direction of propagation, reflection increases the overpressure to a maximum reflected pressure *Pr* as:

$$P_r = 2 * P_{so} * \{\frac{7 * P_o + 4 * P_{so}}{7 * P_o + P_{so}}\} \tag{4.8}$$

Po=14.7

$$P_r = 2 * P_{so} * \{\frac{103 + 4 * P_{so}}{103 + P_{so}}\} \tag{4.9}$$

For design purposes, reflected overpressure can be idealized by an equivalent triangular pulse of maximum peak pressure *Pr* and time duration *td,* which yields the reflected impulse (*ir*).

$$i_r = \frac{1}{2} * P_r * t_d \tag{4.10}$$

Duration td is related directly to the time taken for the overpressure to be dissipated.

Overpressure arising from wave reflection dissipates as the perturbation propagates to the edges of the obstacle at a velocity related to the speed of sound (Vs) in the compressed and heated air behind the wave front. Denoting the maximum distance from an edge as S (for example, the lesser of the height or half the width of a conventional building), the additional pressure due to reflection is considered to reduce from Pr – Pso to zero in time 3S/Vs. Conservatively, Vs can be taken as the normal speed of sound, which is about 340 m/s, and the additional impulse to the structure evaluated on the assumption of a linear decay.

After the blast wave has passed the rear corner of a prismatic obstacle, the pressure similarly propagates on to the rear face; linear build-up over duration 5S/Vs has been suggested.

For skeletal structures the effective duration of the net overpressure load is thus small, and the drag loading based on the dynamic pressure is then likely to be dominant. Conventional wind loading pressure coefficients may be used, with the conservative assumption of instantaneous build-up when the wave passes the plane of the relevant face of the building, the loads on the front and rear faces being numerically cumulative for the overall load effect on the structure.

Various formulations have been put forward for the rate of decay of the dynamic pressure loading.

$$V_s = 1117 * (0.0583 * P_{so} + 1)^{\frac{1}{2}} \tag{4.11}$$

From Fig (a), the positive phase duration ($t_{o1}$) of the overpressure Pso for 1 kiloton weapon yield is given then for estimating the value which needed using as

$$t_{o2} = t_{o1} * (Z^{\frac{1}{3}}) \tag{4.12}$$

The peak dynamic pressure (qs) can be determined from Fig. b. With Pso, the range $d_1$ for a 1-kiloton weapon is given. In the same figure, the same range, the peak dynamic pressure qs is given.

$$d = d_1 * (Z^{(1/3)}) \tag{4.13}$$

The positive phase duration ($t_o d1$) of the dynamic pressure (qs) for 1-kiloton weapon yield can be found from Fig. (c) Thus, with $d_1$, Fig. (c) yields $t_{od1}$ is given

$$t_o d = t_o d1 * (Z^{(1/3)}) \tag{4.14}$$

Pressure on front face of building

$$t_c = \frac{3S}{V_s} \tag{4.15}$$

$$\begin{aligned} t_{o2} &= t_{od} \\ t &= t_c \end{aligned} \tag{4.16}$$

If Pso<10 then we can use these formula

$$P_s = P_{so} * \left[1 - \frac{t}{t_o}\right] * e^{\frac{-t}{t_o}} \tag{4.17}$$

$$P_d = P_{do} * \left[1 - \frac{t}{t_{od}}\right] * e^{\frac{-2t}{t_{od}}} \tag{4.18}$$

$$\begin{aligned} \mathrm{P_{front}} &= P_s + C_1 * P_d \\ C_1 &= 0.85 \end{aligned} \tag{4.19}$$

Pressure on the rear face of building

The time td at which the shock front arrives at the back face of the building is

$$\mathrm{t_d} = \frac{\mathrm{L}}{\mathrm{Vs}} \tag{4.20}$$

The time tb that is required for the average pressure Pback to build up to its maximum value (Pback) max is,

$$\begin{aligned} t_b &= 5S / Vs \\ t &= t_b \\ t_o &= t_{o2} \end{aligned} \tag{4.21}$$

The value Psb of the overpressure

$$P_{sb} = P_{so} * \left[1 - \frac{t}{t_o}\right] * e^{\frac{-t}{t_o}} \tag{4.22}$$

$$\beta = \mathrm{P_{so}} / 2\mathrm{P_o} \tag{4.23}$$

$$P_{back} = \frac{P_{sb}}{2} + [1 + (1 - \beta) * e^{-\beta} \tag{4.24}$$

### *4.2 Numerical Estimation of blast load*

For the modeling there is need of step by step procedure to find the net pressure on the building. The building is assumed to be subjected to weapon yield of W= (1200 kilogram TNT) 1.2 KILLO TNT And R= 5m = 16.4 ft.

W= 1.2 * 2.2 = 2640 lbs

Scaled distance calculated from equation (4.1)

Z=1.2

From figure (4a) we can find value of pressure as below

$P_{so}$ = 5.45 Psi

For computing front velocity equation (4.11) is used

Vs= 1117* [0.0583* Pso + 1] $^{0.5}$ =1283 Ft/sec

To1 = Positive phase duration of the over pressure Pso for the 1 KILOTON weapon yield.

From Fig (4a), the positive phase duration (to1) of the overpressure Pso for 1 kiloton weapon yield is 0.314 sec.

$t_{o2} = t_{o1} * (Z^{\frac{1}{3}})$ = 0.314* (1.2)$^{1/3}$ = 0.33sec

The peak dynamic pressure (qs) can be determined from Fig. (4b). With Pso=5.45 psi, the range d1 for a 1-kiloton weapon is 1400.00 ft. In the same figure, the same range, the peak dynamic pressure qs is 0.65 psi.

For computing peak dynamic pressure we can use direct formula

$q_{(s)} = \frac{{P_{so}}^2}{(0.4p_{so}+41.2)}$ =(5.45)$^2$ /(0.4*5.45+41.2) = 0.68 psi.

$d = d_1 * (Z^{\frac{1}{3}})$ =1400*1.2$^{1/3}$ = 1485ft

The positive phase duration (tod1) of the dynamic pressure (qs) for 1-kiloton weapon yield can be found from Fig.(4c) Thus, with d1=1400 ft, Fig. © yields tod1=0.39 sec.

$t_{od} = t_{od1} * (Z^{\frac{1}{3}})$ =0.39*(1.2)$^{1/3}$ = 0.41 sec

Computation of peak reflected overpressure

$P_r = 2 * P_{so} * \{\frac{7*P_o+4*P_{so}}{7*P_o+P_{so}}\}$ = 2* 5.45* [(7*14.7+4*5.45)/(7*14.7+5.45)]=12.56 psi

$S = \min\left[\frac{B}{2}, \frac{H}{2}\right]$ =min [15/2, 15/2] = 7.5m = 24.6ft

Where S = maximum distance from an edg of building

That is lesser of Height or width of the building

$t_c = \frac{3S}{V_s}$ = 3*24.6/1283 =0.0575 sec

Pressure on front face of building

$t_{o2} = t_{od}$= 0.33sec

$t = t_c$ =0.0575 sec

Because Pso<10 then these formula are used

$P_s = P_{so} * \left[1 - \frac{t}{t_o}\right] * e^{\frac{-t}{t_o}}$ = 3.78 psi

$P_d = P_{do} * \left[1 - \frac{t}{t_{od}}\right] * e^{\frac{-2t}{t_{od}}}$ = 0.5827 psi

$P_{front}$ = 3.78+0.850*0.5827= 4.25 psi

Pressure on the rear face of building

The time td at which the shock front arrives at the back face of the building is

$t_d$ = L/Vs = 49.2/1283 = 0.0383 sec

The time tb that is required for the average pressure Pback to build up to its maximum value (Pback) max is,

$t_b$ = 5S/Vs = 5* 24.6/1283 = 0.9586 sec

With t = tb = 0.09586 sec and to = to2 =0.33 sec, the value Psb of the overpressure

$P_{sb} = P_{so} * \left[1 - \frac{t}{t_o}\right] * e^{\frac{-t}{t_o}}$ = 2.89 psi

$\beta = P_{so}/2P_o$ = 0.5*5.45/14.7 = 0.186

$P_{back} = \frac{P_{sb}}{2} + [1 + (1 - \beta) * e^{-\beta}$ = 3.12 psi

$P_{net} = P_{front} - P_{back}$ = 4.275 - 3.12= 1.155 psi= 7.96 KN/$m^2$

Say $P_{net}$ = 8KN/$m^2$

**Estimation for Blast Pressure for R = 10mtr.**

The step by step procedure for finding net pessure on the building.

| | | | | | | | |
|---|---|---|---|---|---|---|---|
| The Building is assumed to be subjected to weapon yeild of | | | | | | **1.20** | kiloton |
| W | | | | | | **2640.0** | lbs |
| R | | | 10 | mtr | | **32.80** | feet |
| Scaled distance | | | Z | = | R/(W⅓) | **2.44** | |
| Pso = | (0.975/Z) + | (1.455/Z^2) + | (5.85/Z^3) - | 0.2755 | | | |
| | | | = | 0.4686 | | | |
| Pso | | | | | | **0.4686** | psi |
| Front Velocity (Vs) | | = | | 1117X(0.0583XPso+1)^1/2 | | | |
| | | = | | | | **1132** | Ft. |
| Positive phase duration (to1) of the overpressure Pso for 1 kiloton weapon yeild is | | | | | | **0.314** | Seconds. |
| to2 | = | to1 X (Z^1/3) | | | | **0.421** | Seconds. |
| The peak dynamic pressure can be calculated as under | | | | | | | |
| qs | = | Pso^2/(0.4Pso+41.2) | | | | **0.0053** | |
| d | = | d1 X (Z^1/3) | | | | | |
| where d1 | = | positive phase duration (to1) of the dynamic pressure (qs) for 1 kiloton weapon yeild , can found from graph | | | | **1400** | ft. |
| tod1 | | | | (Refer Graph) | | **0.39** | Seconds |
| tod | = | to1 X (Z^1/3) | | | | **0.469** | |
| Computation of peak reflected overpressure | | | | | | | |
| Pr | = | 2XPsoX{(7XPo+4XPso)/(7XPo+Pso)} | | | | | |
| where | Po | = | | | | 14.7 | |
| | Pr | = | | | | **0.9499** | psi |
| | S | = | | min[B/2,H/2] | | | |
| where | B | = | | Breadth of building | | 15 | mtr |
| | H | = | | Height of building | | 15 | Mtr |

| | | | | | |
|---|---|---|---|---|---|
| Therefore S = | | | | **7. 5** | Mtr |
| | | | | 24.6 | Feet |
| tc | = | 3S/Vs | | **0.0651** | Seconds |
| to2 = | tod= | | | **0.42** | Seconds |
| t = | tc | | | **0.0651** | Seconds |

Because Pso is less than 10, we can use these formula

| | | | |
|---|---|---|---|
| Ps = | Pso X [1-t/tc] X e^(-tc/to2) | **0.3391** | Psi |
| where Pdo is | | 1.0 | |
| Pd = | Pdo X [1-(t/tod)]Xe^(-2t/tod) | **0.62** | Psi |

| | | | | | |
|---|---|---|---|---|---|
| P front | = | Ps + (C1 X Pd) | | | |
| | where C1 | = | 0.85 | | |
| P Front | = | | | **0.867** | psi |

<u>Pressure on the Rear face of the building</u>

(td) The time at which the shock front arrives at the back face of the building is

| | | | |
|---|---|---|---|
| td = | L/Vs | **0.0434** | Seconds |
| | where L is Length of the building | | |

(tb) The time tb that is required for the average pressure P'back' to build up to its maximum value P 'back' max is

| | | | | | |
|---|---|---|---|---|---|
| tb = | 5 | S/Vs | | **0.109** | seconds |
| with t = tb = | | 0.109 | seconds | | |
| to = to2 | | | | | |
| = | | 0.419 | seconds | | |

the value of the (Psb) of the overpressure

| | | | |
|---|---|---|---|
| Psb = | Pso X [1-tb/to] X e^(-tc/to) | **0.2676** | |
| ß = | Pso/2Po | **0.0159** | |
| Pback = | (Psb/2) + (1 + (1 -ß) X (e^-ß) | **2.101** | psi |
| Pnet = | Pfront - Pback | **-1.23** | psi |
| | | **-8.47** | kN/sqm |

**Calculation for Blast Pressure at R=20m**

| | | | | | | |
|---|---|---|---|---|---|---|
| The step by step procedure for finding net pessure on the buiding. | | | | | | |
| The Building is assumed to be subjected to weapon yeild of | | | | | 1.20 | kilotnt |
| W | | | | | 2640.00 | lbs |
| R | | 20 | mtr | | 65.60 | feet |
| Scaled distance | | Z | = | R/(W⅓) | 4.87 | |
| Pso = | (0.975/Z) + | (1.455/Z^2) + | (5.85/Z^3 | -0.2755 | | |
| | 0.20536261 | 0.064550037 | 0.0546646 | | | |
| | | = | 0.2692 | | | |
| Pso | | | | | 0.2692 | Psi |
| Front Velocity (Vs) | | = | 1117X(0.0583XPso+1)^1/2 | | | |
| | | = | | | 1126.00 | feet |
| Positive phase duration (to1) of the overpressure Pso for 1 kiloton weapon yeild is | | | | | 0.314 | seconds |
| to2 | = | to1 X (Z^1/3) | | | 0.529 | seconds |
| The peak dynamic pressure can be calculated as under | | | | | | |
| qs | = | Pso^2/(0.4Pso+41.2) | | | 0.001754 | |
| d | = | d1 X (Z^1/3) | | | | |
| where d1 | = | postive phase duration (to1) of the dynamic pressure (qs) for 1 kiloton weapon yeild , can found from graph | | | 1400 | Ft. |
| tod1 | | (Refer Graph) | | | 0.39 | seconds |
| tod | = | to1 X (Z^1/3) | | | 0.655 | seconds |
| Computation of peak reflected overpressure | | | | | | |
| Pr | = | 2XPsoX{(7XPo+4XPso)/(7XPo+Pso)} | | | | |
| where | Po | = | | | 14.7 | |
| | Pr | = | | | 0.5426 | Psi |
| | S | = | min[B/2,H/2] | | | |

| | | | | | | |
|---|---|---|---|---|---|---|
| where | B | = | Breadth of building | | 15 | Mtr |
| | H | = | Height of building | | 15 | Mtr |
| Therefore | S = | | | | 7.5 | Mtr |
| | | | | | 24.6 | Feet |
| tc | | = | 3S/Vs | | 0.0655 | seconds |
| to2 = | tod= | | | | 0.53 | seconds |
| t = | Tc | | | | 0.06554 | seconds |

Because Pso is less than 10, we can use these formula

| | | | | | | |
|---|---|---|---|---|---|---|
| Ps = | Pso X [1-t/tc] X e^(-tc/to2) | | | | 0.2085 | psi |
| where | Pdo is | | | | 1.0 | |
| Pd = | Pdo X [1-(t/tod)]Xe^(-2t/tod) | | | | 0.6844 | psi |
| P front | = | Ps +(C1 x Pd) | | | | |
| | where C1 | = | 0.85 | | | |
| | | | | | 0.70 | psi |

Pressure on the Rear face of the building

(td) The time at which the shock front arrives at the back face of the building is

| | | | | | | |
|---|---|---|---|---|---|---|
| td = | L/Vs | | | | 0.436 | seconds |
| | where L is Length of the building | | | | | |

(tb) The time tb that is required for the average pressure P'back' to build up to its maximun value P 'back' max is

| | | | | | | |
|---|---|---|---|---|---|---|
| tb = | 5 | S/Vs | | | 0.109 | Seconds |
| with t = tb = | | 0.293 | Seconds | | | |
| to = to2 | | | | | | |
| = | | 0.528 | Seconds | | | |

the value of the (Psb) of the overpressure

| | | | | | | |
|---|---|---|---|---|---|---|
| Psb = | Pso X [1-tb/to] X e^(-tc/to) | | | | 0.1888 | psi |
| ß = | Pso/2Po | | | | 0.00915 | |
| Pback = | (Psb/2) + (1 + (1 -ß) X (e^-ß) | | 0.006256 | 1.998 | 2.06 | |
| Pnet = | Pfront - Pback | | | | -1.30 | Psi |
| | | | | | - 8.75 | kN/sqm |

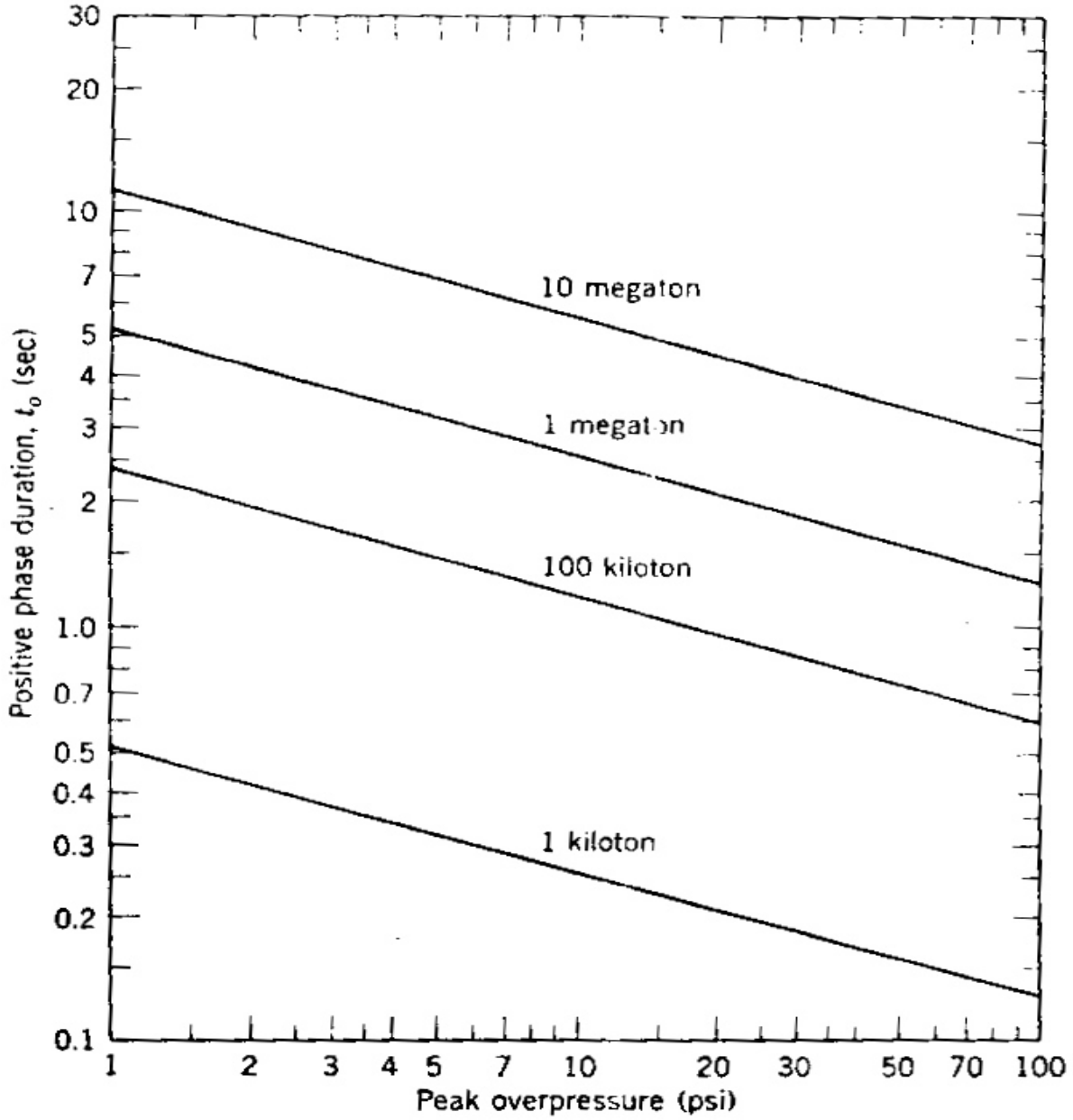


Figure 4a Positive phase duration of overpressure for surface burst (Mays GC and Smith PD (2001) Blast Effects on Buildings).

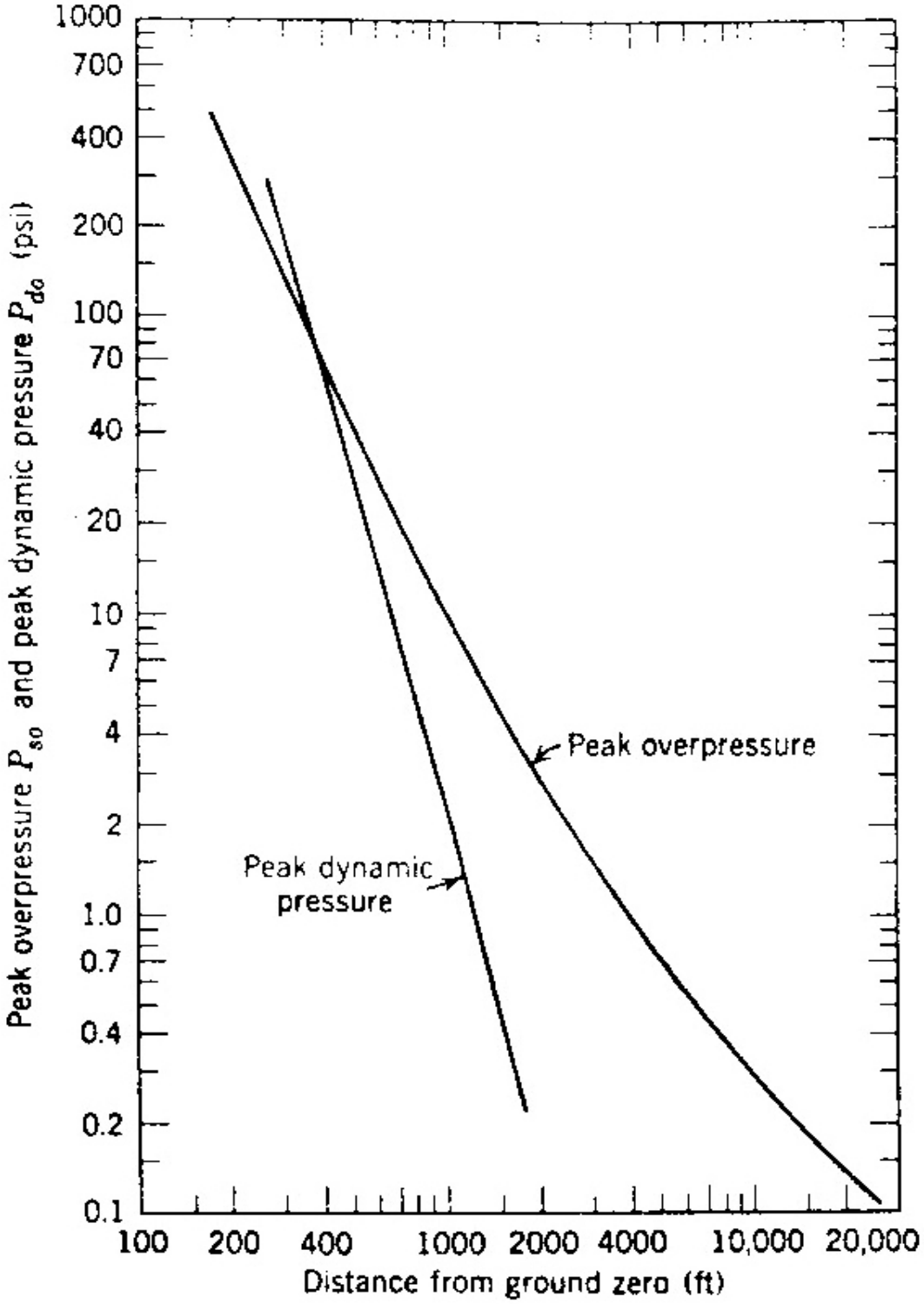


Figure 4b Peak overpressure and peak dynamic pressure for surface burst (Mays GC and Smith PD (2001) Blast Effects on Buildings).

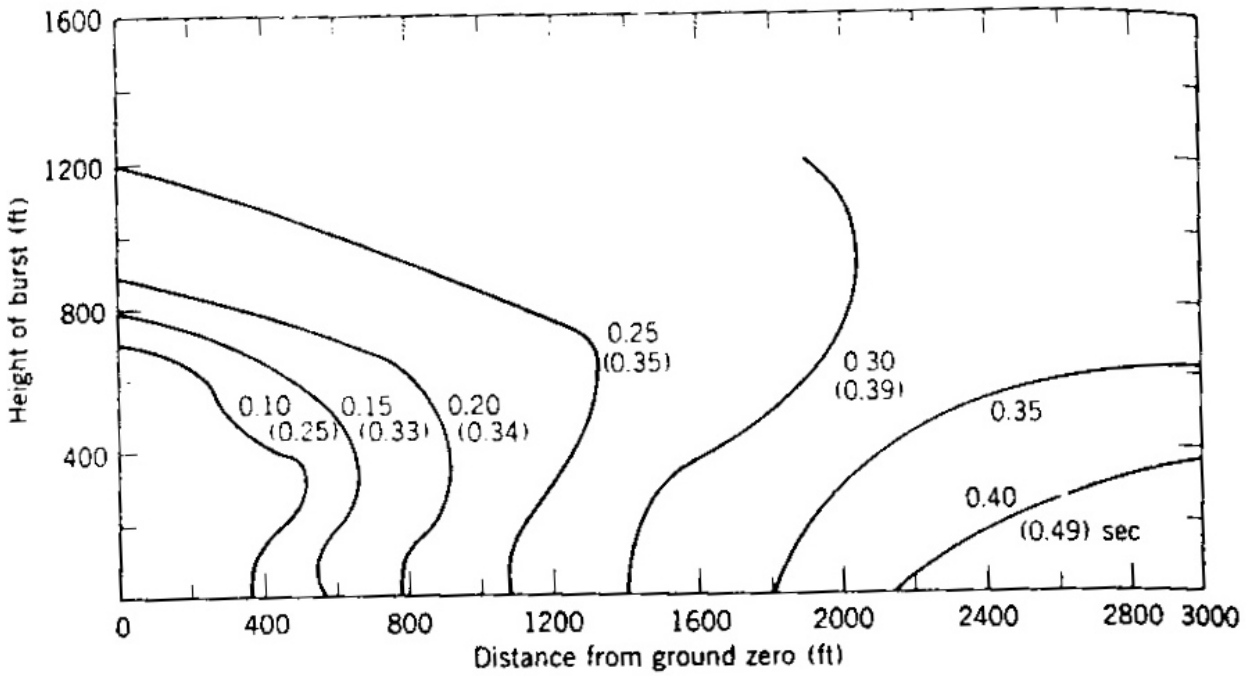


Figure 4c Positive phase duration of overpressure and dynamic pressure (Mays GC and Smith PD (2001) Blast Effects on Buildings).

The effect of Blast decreases as scale distance increases:

| Sr. No. | Scale Distance (Z) | Distance of building from Blast (R) in meter | P front in Psi | P back in Psi | P net in Psi |
|---|---|---|---|---|---|
| 1. | 1.2 | 5 | 4.25 | 3.12 | 1.155 |
| 2. | 2.44 | 10 | .867 | 2.101 | -1.23 |
| 3. | 3 | 20 | 0.70 | 2.06 | -1.36 |

CHAPTER 5

# EVALUATION OF BUILDING USING ETABS

***The Building as per plan shown below has been evaluated for effect of blast***

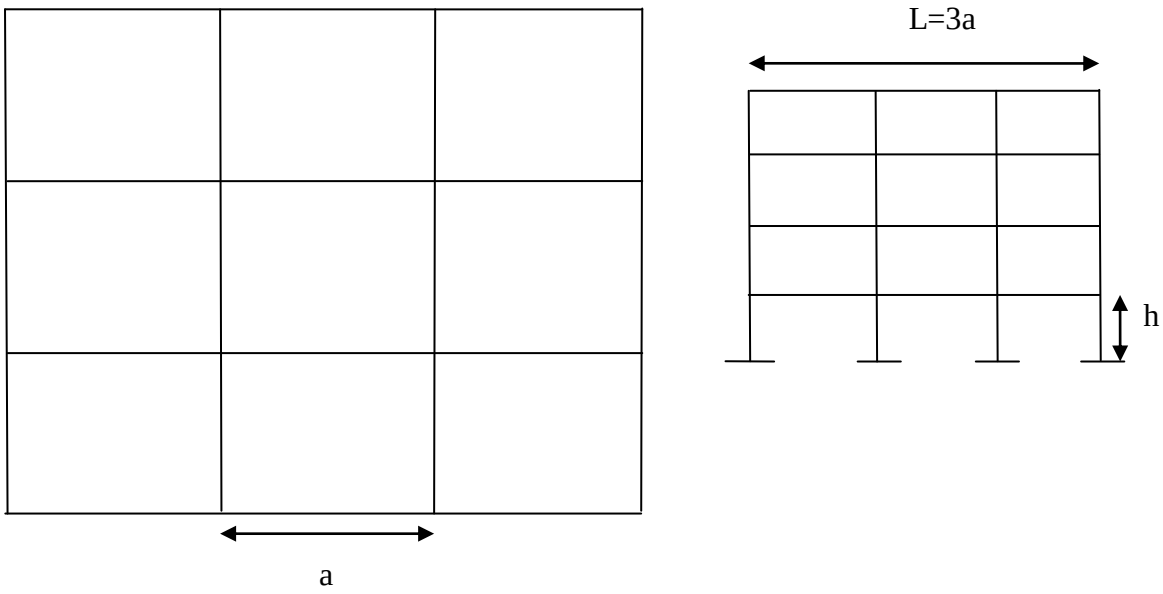


Figure 5A Plan and elevation of the bench mark building

## *5.1 Modeling by software ETABS*

For the modeling of multistory building by ETABS following steps are followed :

### 5.1.1 Begin a New Model

In this Step, the dimensions and story height are set. Then a list of sections that fit the parameters set by the architect for the design is defined.

a- Start the program and click the X on the Tip of the Day window to close it. If the units shown in the drop-down list in the lower right-hand corner of the ETABS window are not KN-m, click the drop-down list to set the units to KN-m.

b- Click the **File menu > New Model** command or the **New Model** button.

c- Select the **No** button on that form.

The Building Plan Grid System and Story Data form is used to specify horizontal grid line spacing, story data, and, in some cases, template models. Template models provide a quick, easy way of starting a model. They automatically add structural objects with appropriate properties to the model.

d- Set the number of stories in the Number of Stories edit box to 4.

e- Type **3.75-m** into the Bottom Story Height edit box and press the Enter key on your keyboard (be sure you type ***m***).

f- . Select the **Grid only** button.

g- Click the **OK** button to accept your selections.

When you click the **OK** button, the model appears on screen in the main ETABS window with two view windows tiled vertically, a Plan View on the left and a 3-D View on the right. The number of view windows can be changed using the **Options menu > Windows** command.

When the window is active, the display title bar is highlighted. Set a view active by clicking any-where in the view window. If you change the views, return to the default described in the previous paragraph, with the Plan

### 5.1.2 Assigning parameter

The material property, section property is defined.

Step 1

click define menu and then material property for defining them

Step 2

After defining material need is to define cross-section for defrent sections such as beam, column, for that define menu then for beams and columns select frame section and after selcting add rectangular section both can be define seperatly.

Step 3

We have to draw the sections by clicking menu of draw and using draw line object type for beams and columns.

Design Parameters:

1. Length of Building = 15 mtr.
2. Breadth of Building = 15 mtr.
3. Size of Columns – 0.5x0.5 m
4. Size of Beams- 0.25x0.4m
5. Height of Each Storey-3.75m
6. Concrete-M30
7. Steel-Fe500
8. Earthquake Zone –V

   Loads:

   1. DL=10KN/m2
   2. LL=2.5KN/m2
   3. Blast Load= 8 KN/m2

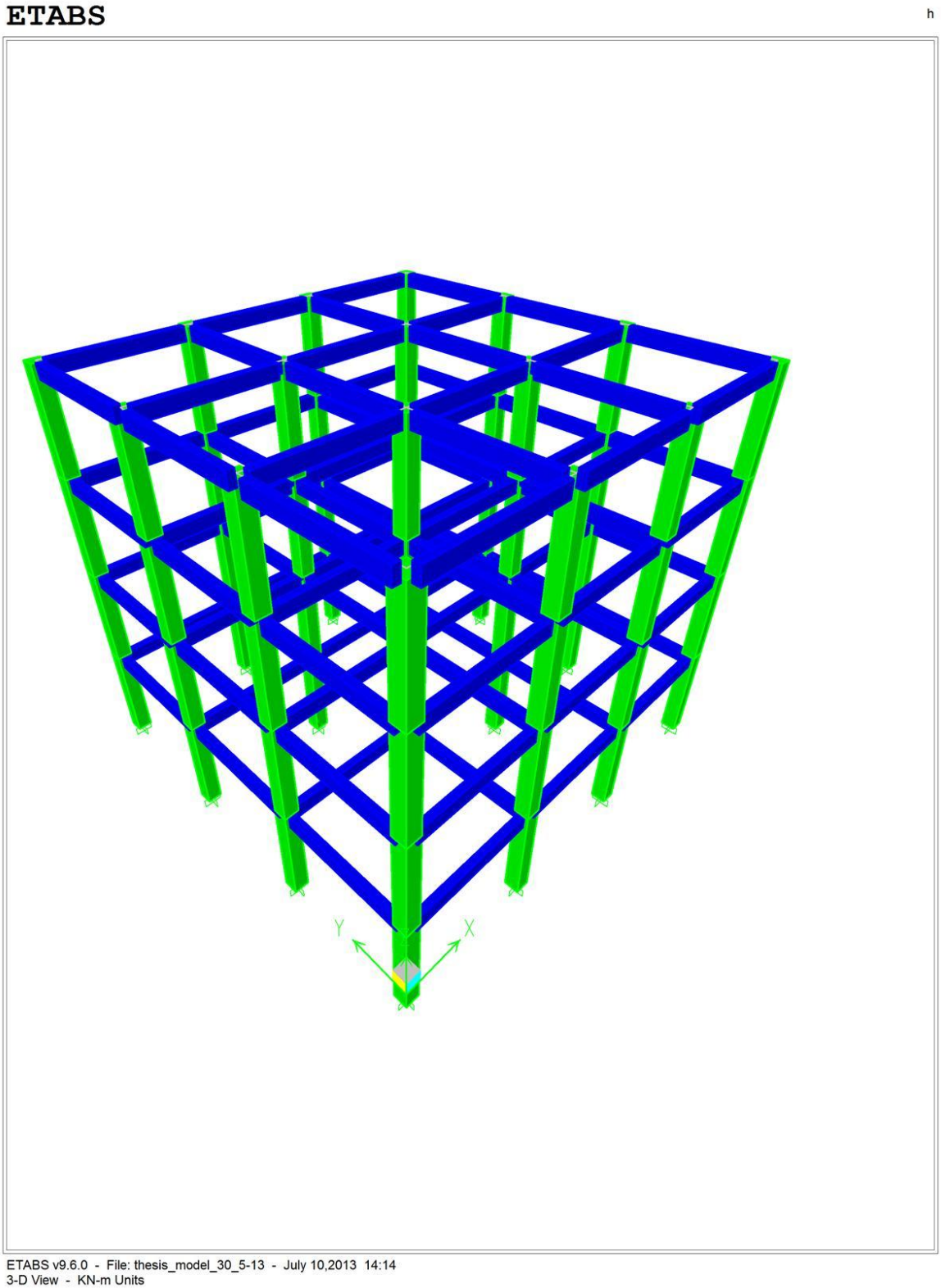


**FIG. 5 B 3-D view of the building**

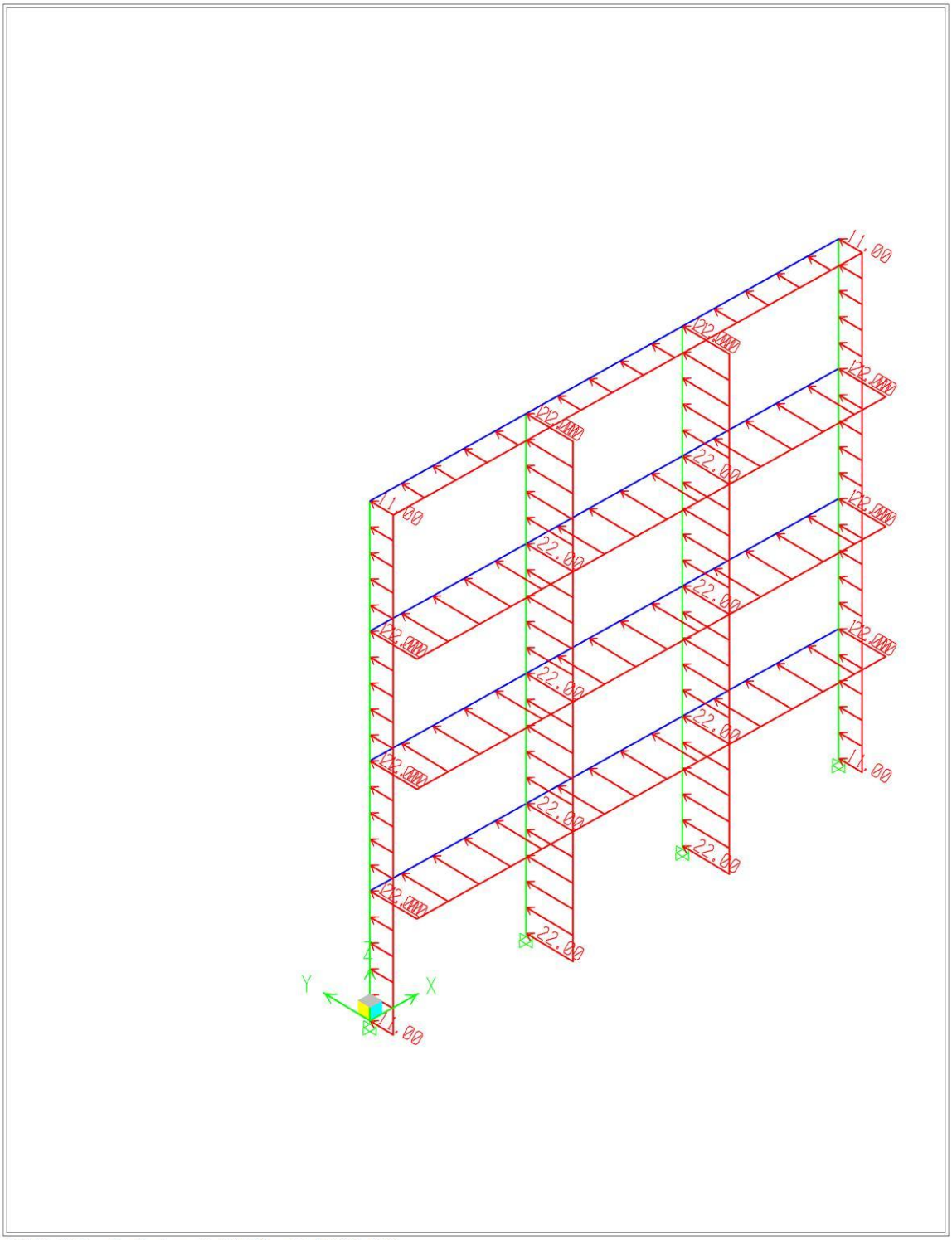


**FIG. 5 C Blast Load on building**

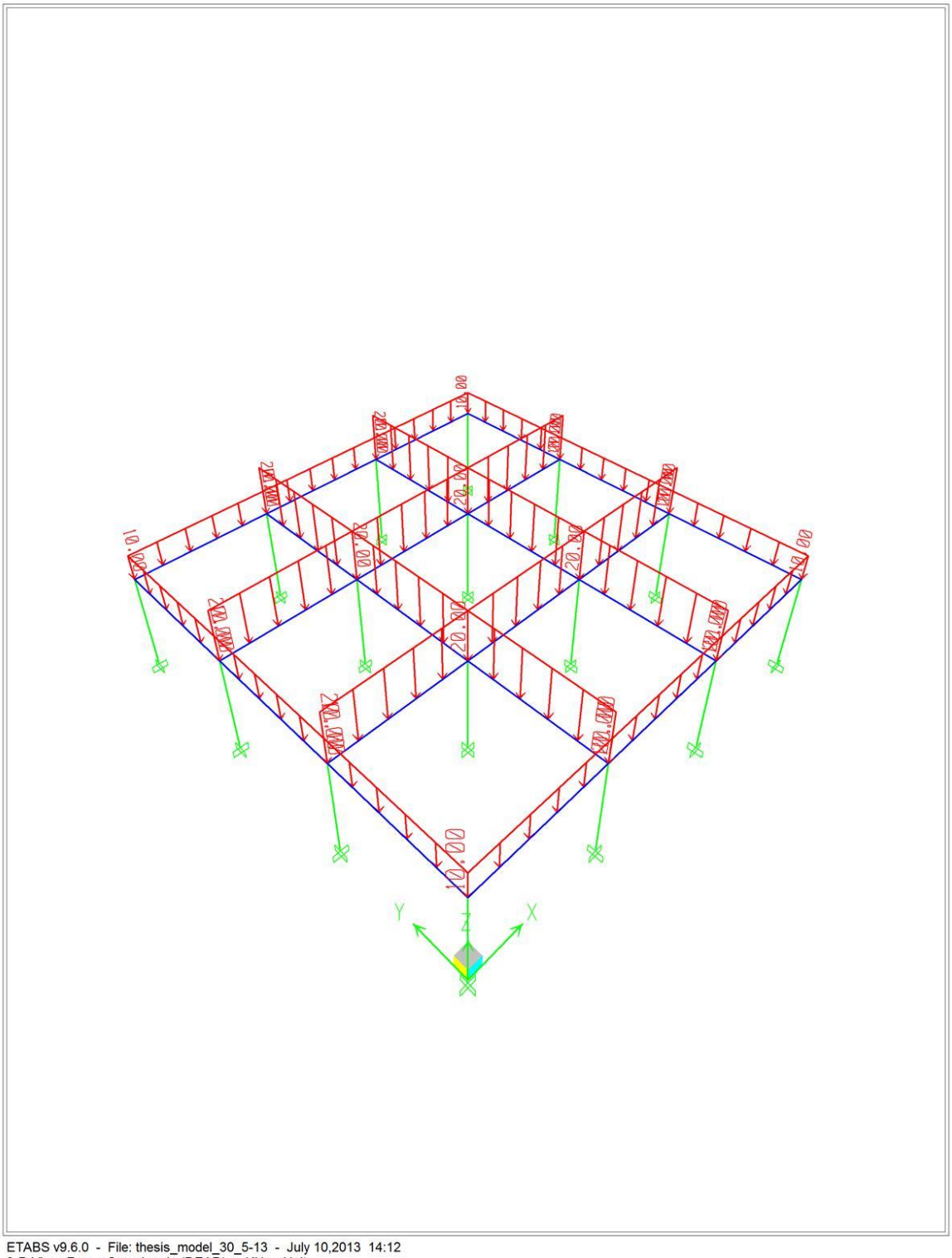


**FIG. 5 D Dead Load on building**

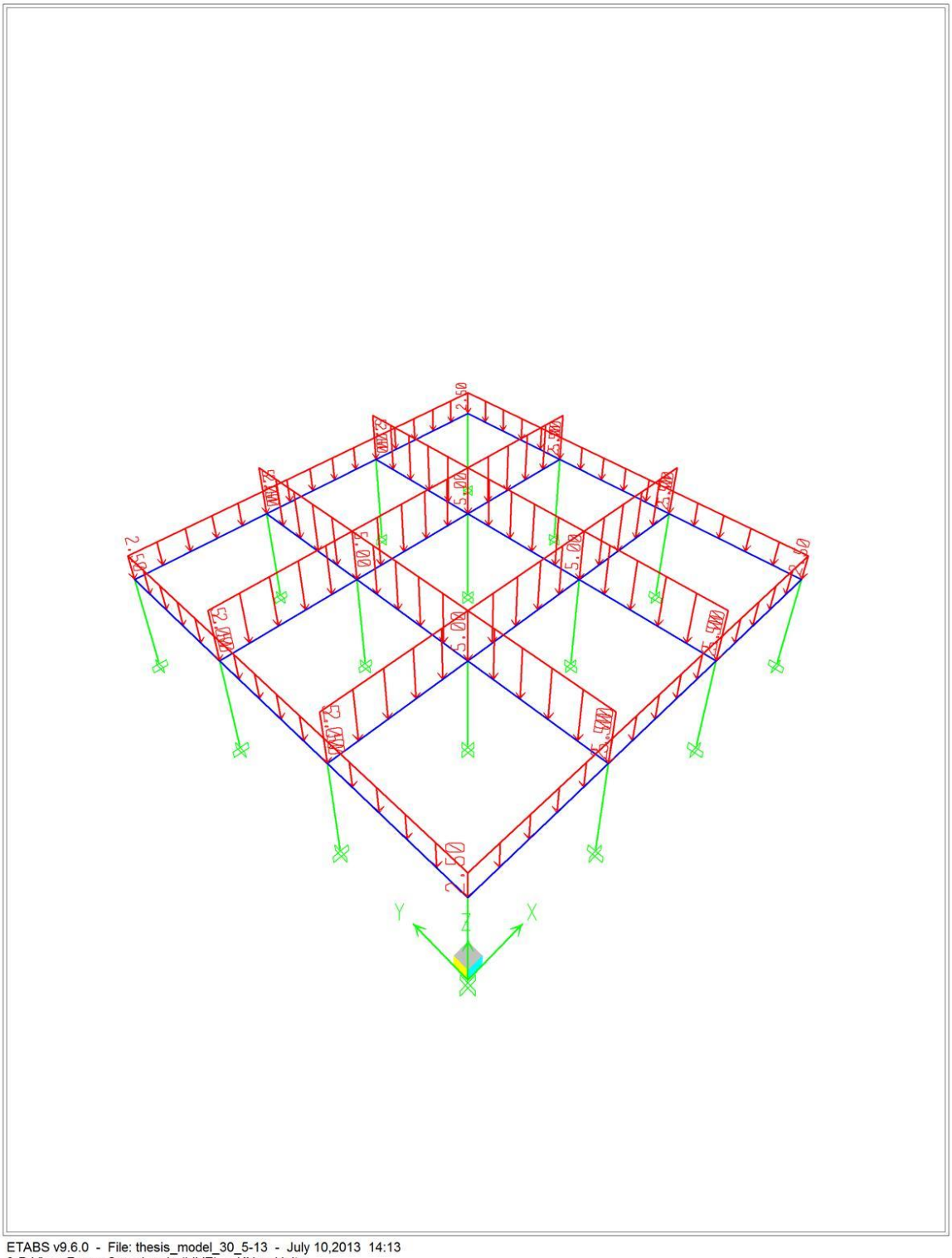


**FIG. 5 E Live Load on building**

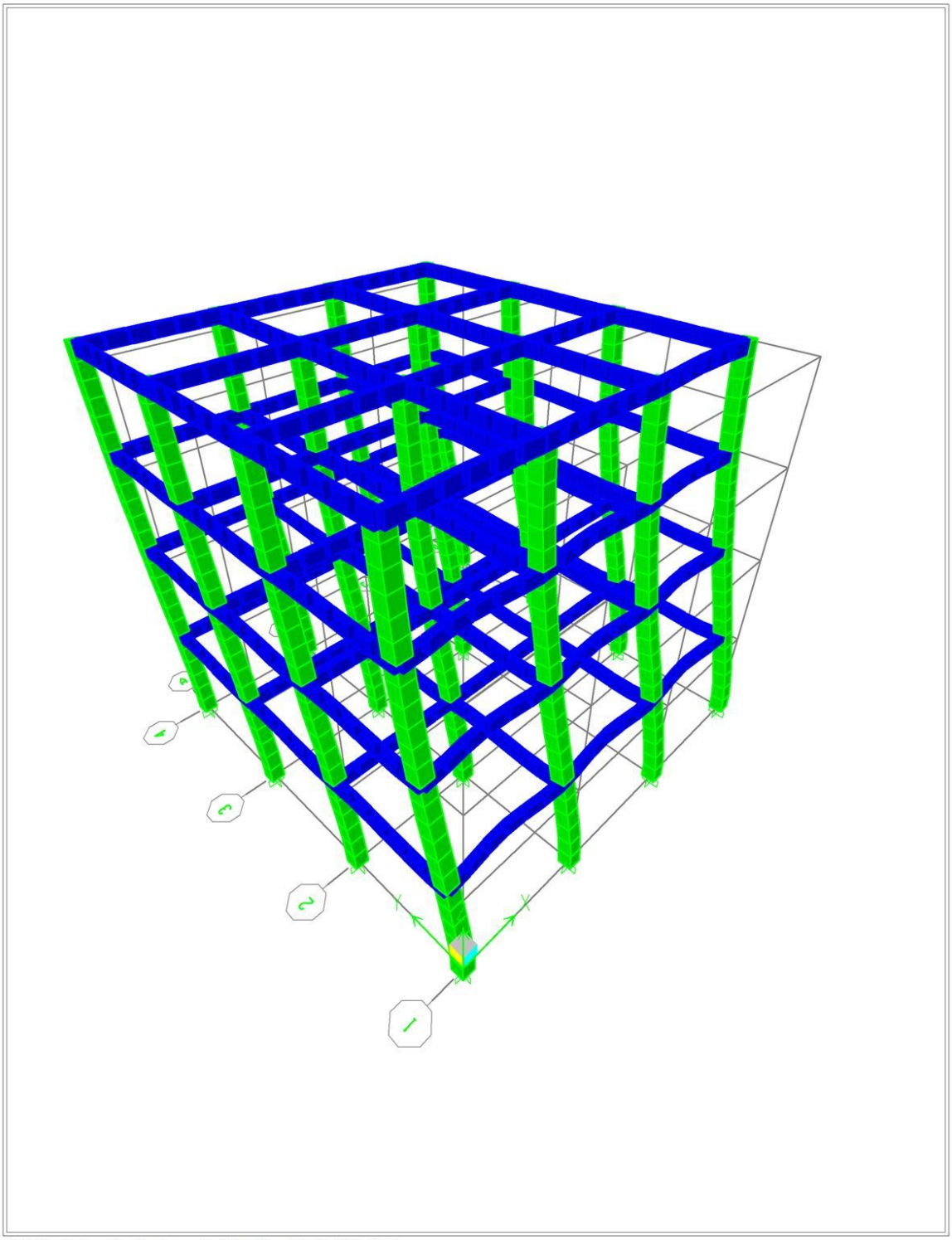


**FIG. 5 F Deformed Shape of the Building in 3-D**

## Mode Shapes

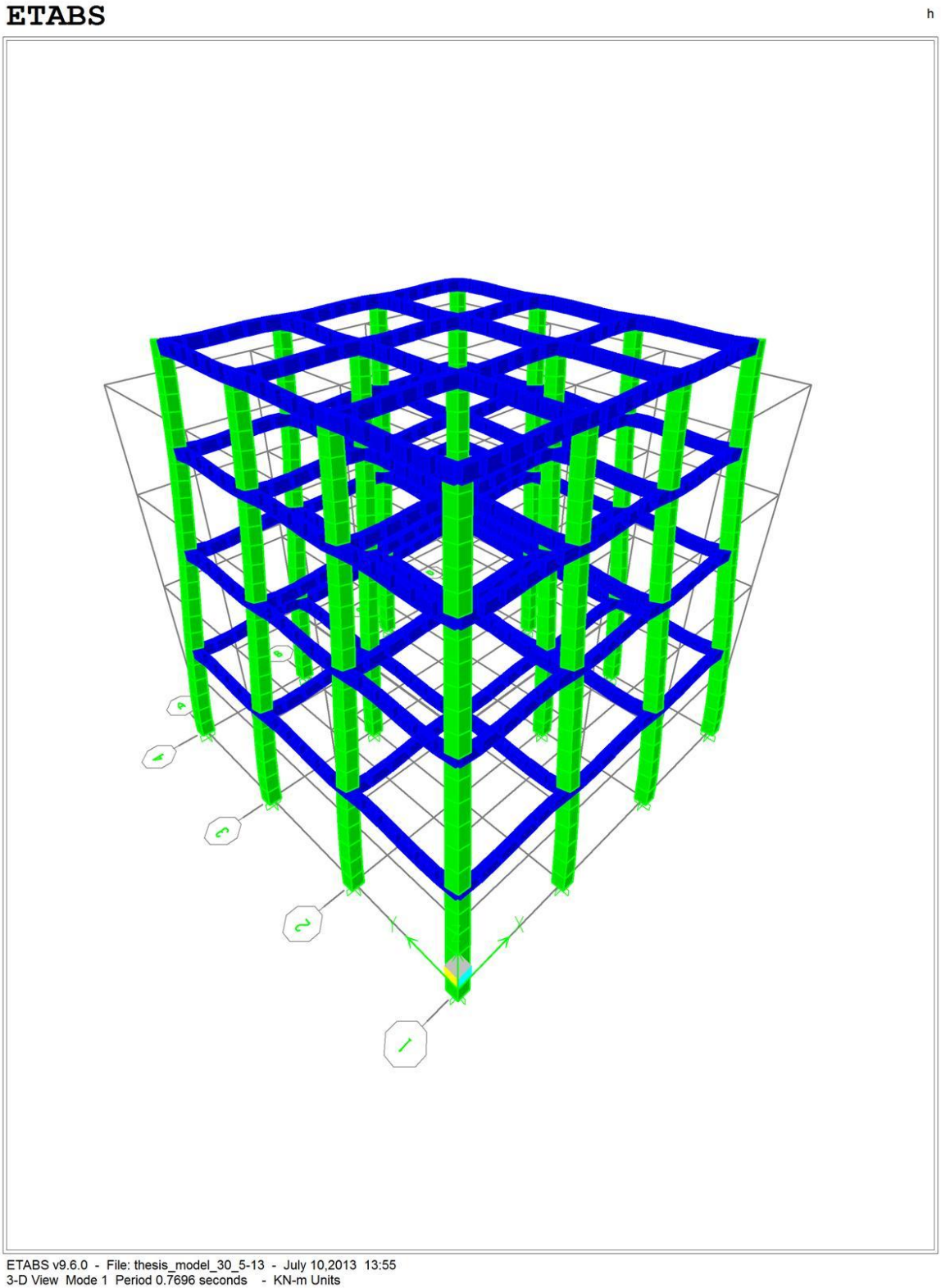


**FIG. 5 G Mode 1 Due to Shear**

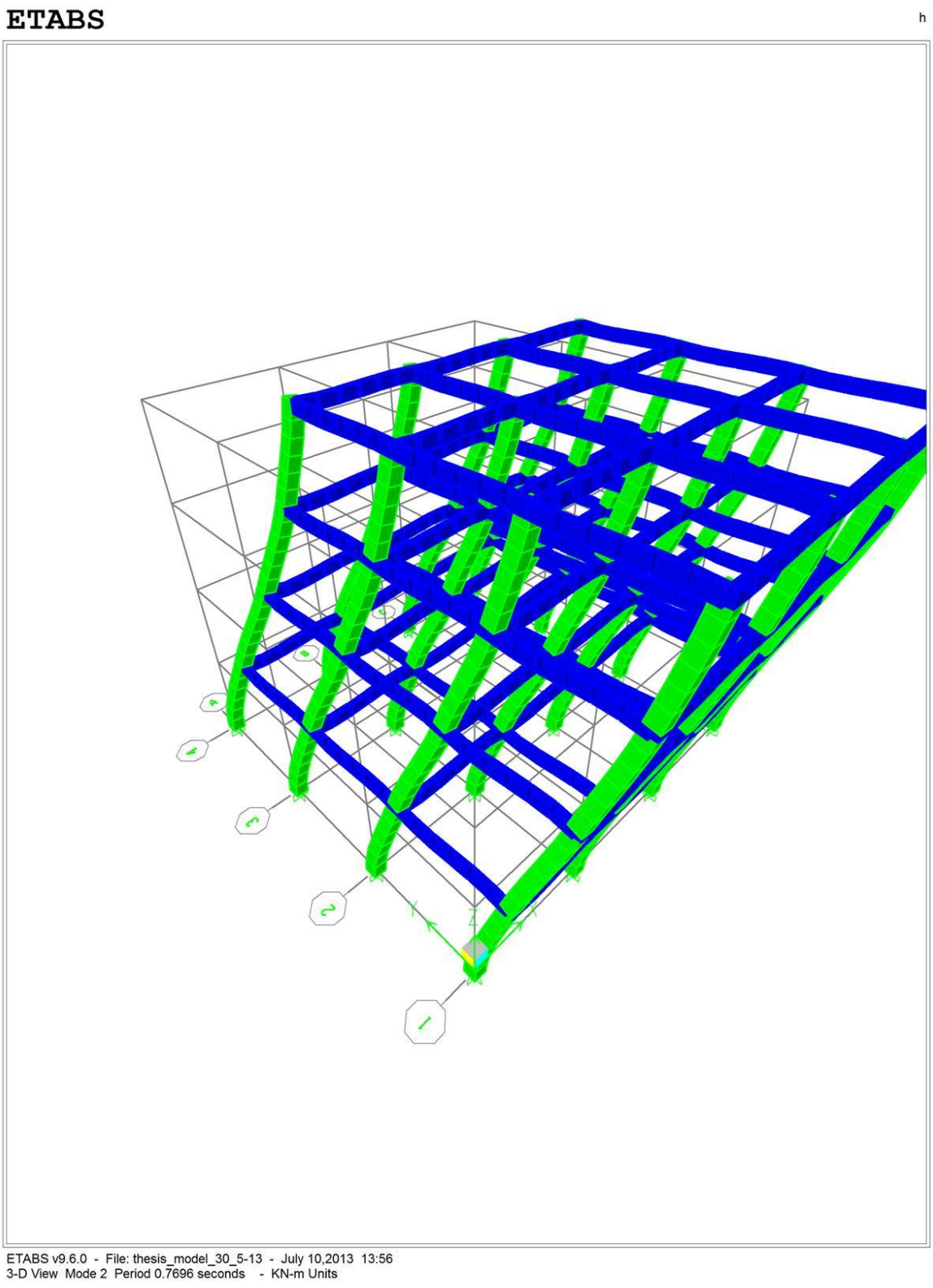


**FIG. 5 H Mode 2 Due to moment**

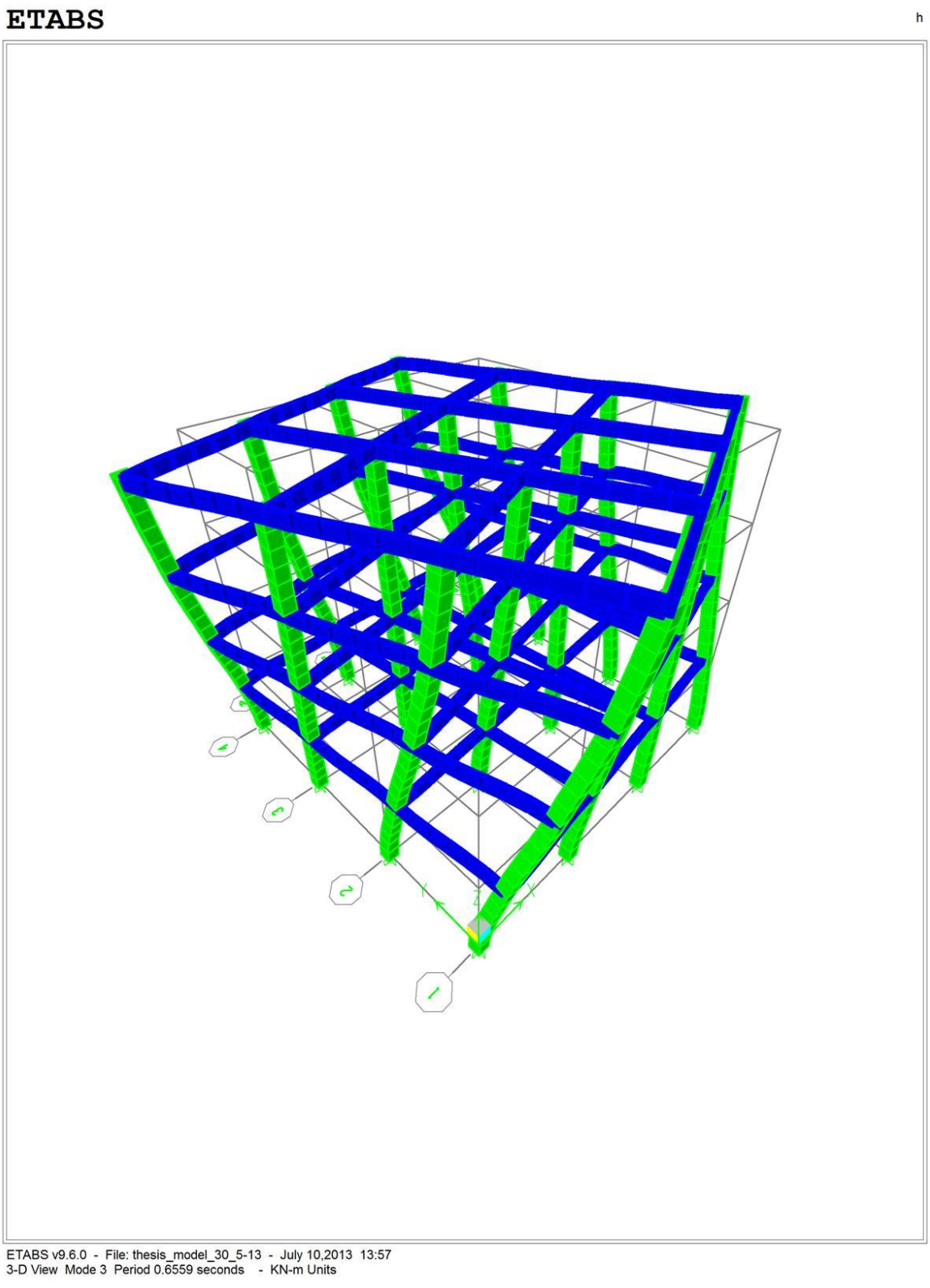


**FIG. 5 I Mode 3 Due to Torsion**

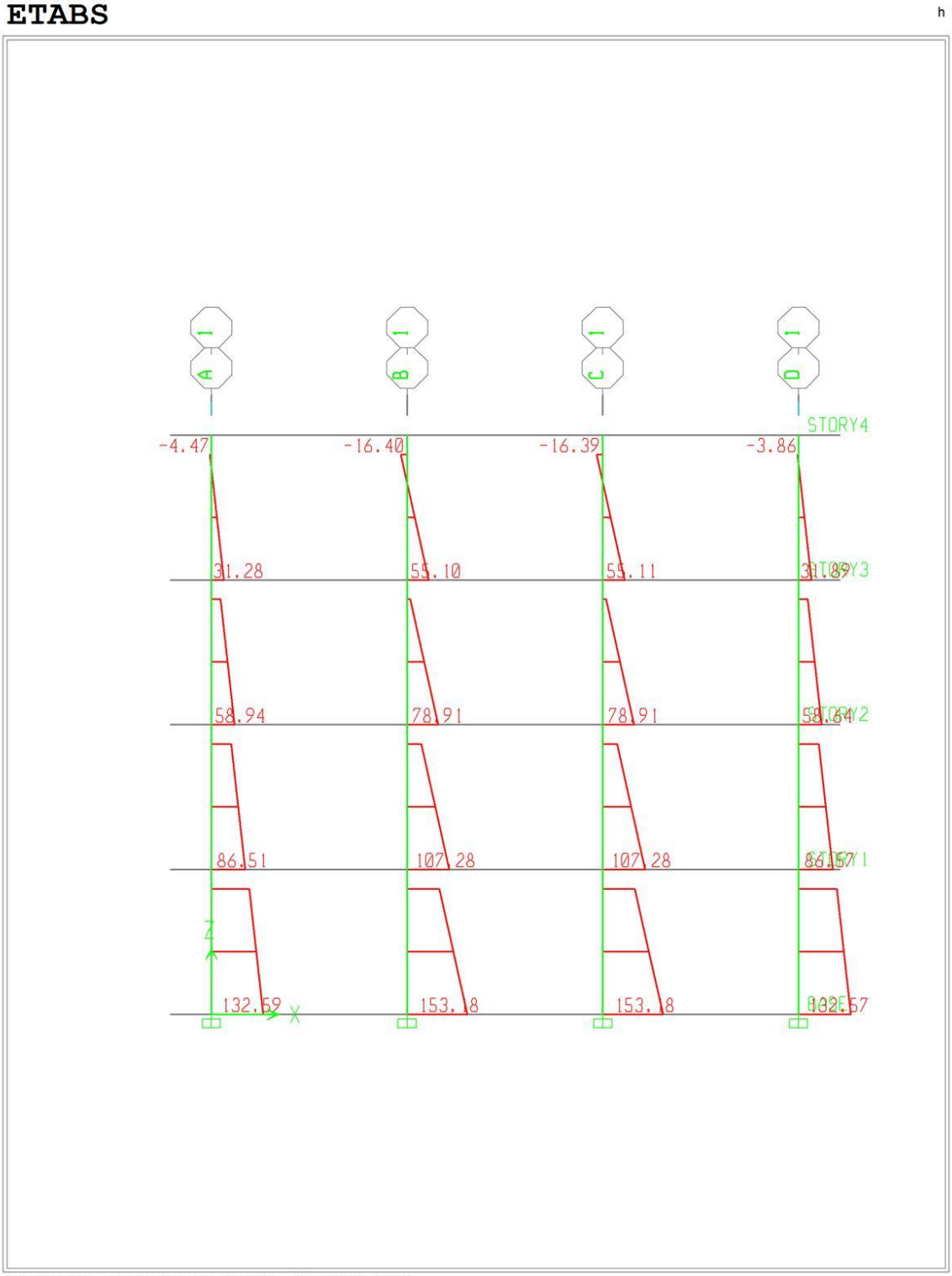


**FIG. 5 J Shear Force Diagram of Columns**

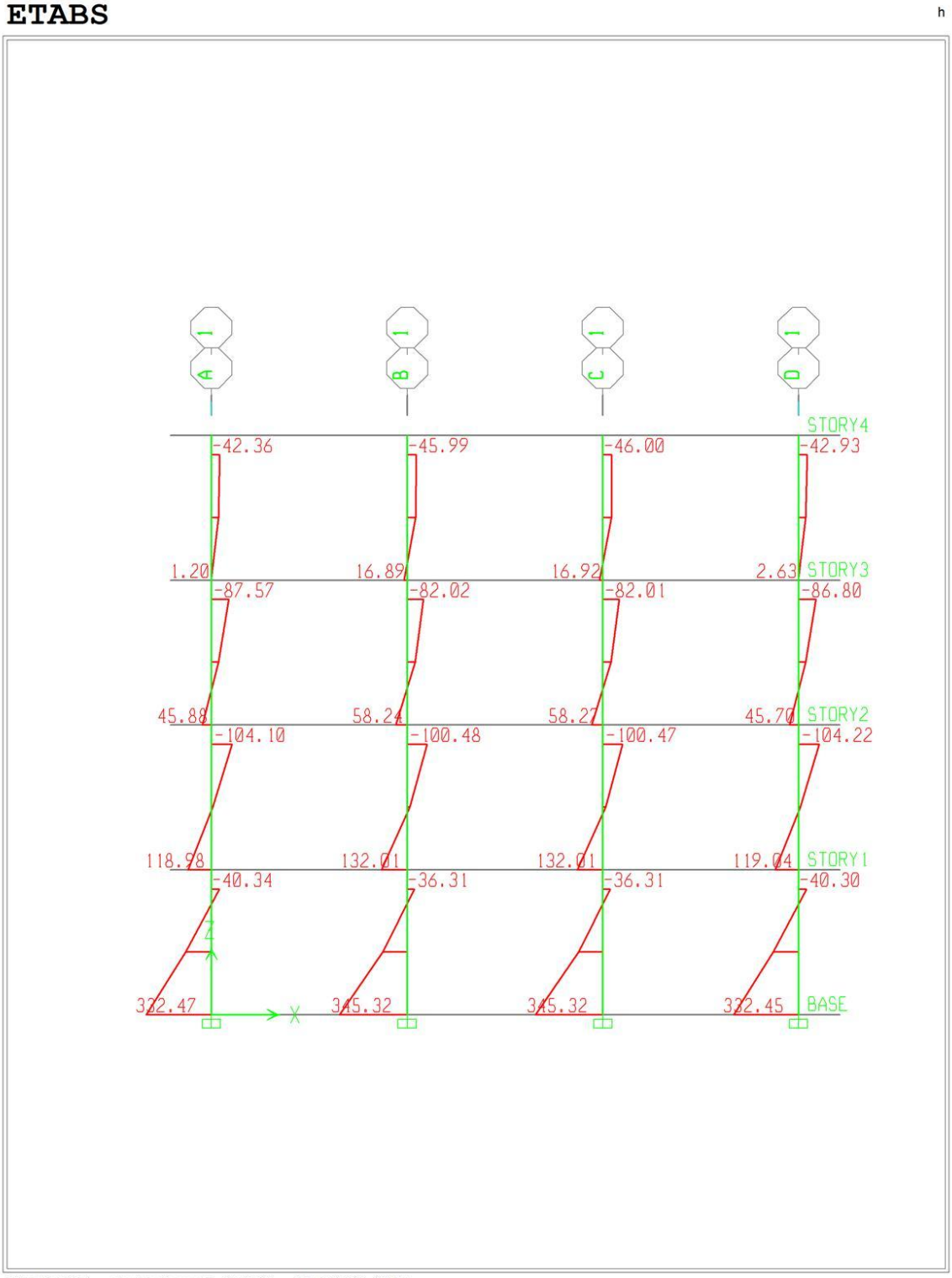


**FIG. 5 K Moment Diagram of Columns**

## Story Drifts

| Story | Load | DriftY | | Story | Load | DriftY |
|---|---|---|---|---|---|---|
| STORY4 | BLAST | 0.001096 | | STORY4 | EQY | 0.000863 |
| STORY3 | BLAST | 0.002246 | | STORY3 | EQY | 0.001273 |
| STORY2 | BLAST | 0.003223 | | STORY2 | EQY | 0.001394 |
| STORY1 | BLAST | 0.002408 | | STORY1 | EQY | 0.000853 |

## Shear Force and Moment Due to Blast

| Story | Load | P (KN) | VX (KN) | VY (KN) | T (KN.m) | MX (KN.m) | MY (KN.m) |
|---|---|---|---|---|---|---|---|
| STORY4 | BLAST | 0 | 0 | -412.5 | -3093.75 | 1082.812 | 0 |
| STORY3 | BLAST | 0 | 0 | -990 | -7425 | 4331.25 | 0 |
| STORY2 | BLAST | 0 | 0 | -1567.5 | -11756.3 | 9745.312 | 0 |
| STORY1 | BLAST | 0 | 0 | -2145 | -16087.5 | 17325 | 0 |

## Shear Force and Moment Due to Earthquake Load

| Story | Load | P (KN) | VX (KN) | VY (KN) | T (KN.m) | MX (KN.m) | MY (KN.m) |
|---|---|---|---|---|---|---|---|
| STORY4 | EQY | 0 | 0 | -329.84 | -2473.79 | 1236.894 | 0 |
| STORY3 | EQY | 0 | 0 | -529.14 | -3968.53 | 3221.159 | 0 |
| STORY2 | EQY | 0 | 0 | -617.71 | -4632.86 | 5537.59 | 0 |
| STORY1 | EQY | 0 | 0 | -639.86 | -4798.94 | 7937.062 | 0 |

## Comparison of Shear Force Moment and Torsion due to Blast Load and EQY Load

| Story | Shear Force Due to Blast Load VY (KN) | Shear Force Due to EQY Load VY (KN) | Moment Due to Blast Load MX (KN.m) | Moment due to EQY Load MX (KN.m) | Torsion due to Blast Load T (KN.m) | Torsion due to EQY Load T (KN.m) | Ratio |
|---|---|---|---|---|---|---|---|
| STORY4 | -412.5 | -329.84 | 1082.812 | 1236.894 | -3093.75 | -2473.79 | 1.25 |
| STORY3 | -990 | -529.14 | 4331.25 | 3221.159 | -7425 | -3968.53 | 1.87 |
| STORY2 | -1567.5 | -617.71 | 9745.312 | 5537.59 | -11756.3 | -4632.86 | 2.53 |
| STORY1 | -2145 | -639.86 | 17325 | 7937.062 | -16087.5 | -4798.94 | 3.35 |

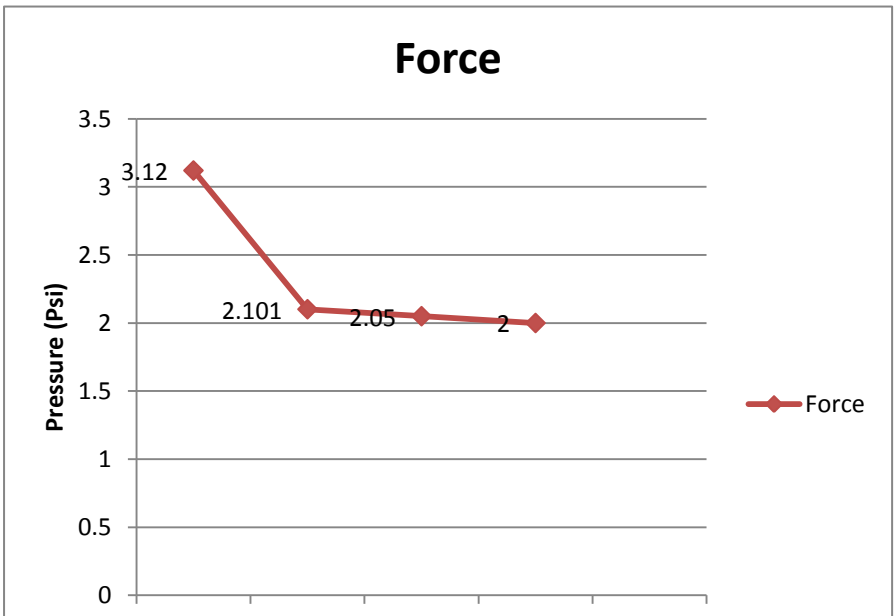

| Distance in Meter | P front in Psi |
|---|---|
| 5 | 4.25 |
| 10 | 0.86 |
| 15 | 0.75 |
| 20 | 0.7 |
| | |

**FIG. 5 L The Graph showing front pressure on the Building due to Blast**

| Distance in meter | P back in Psi |
|---|---|
| 5 | 3.12 |
| 10 | 2.101 |
| 15 | 2.05 |
| 20 | 2 |
| | |

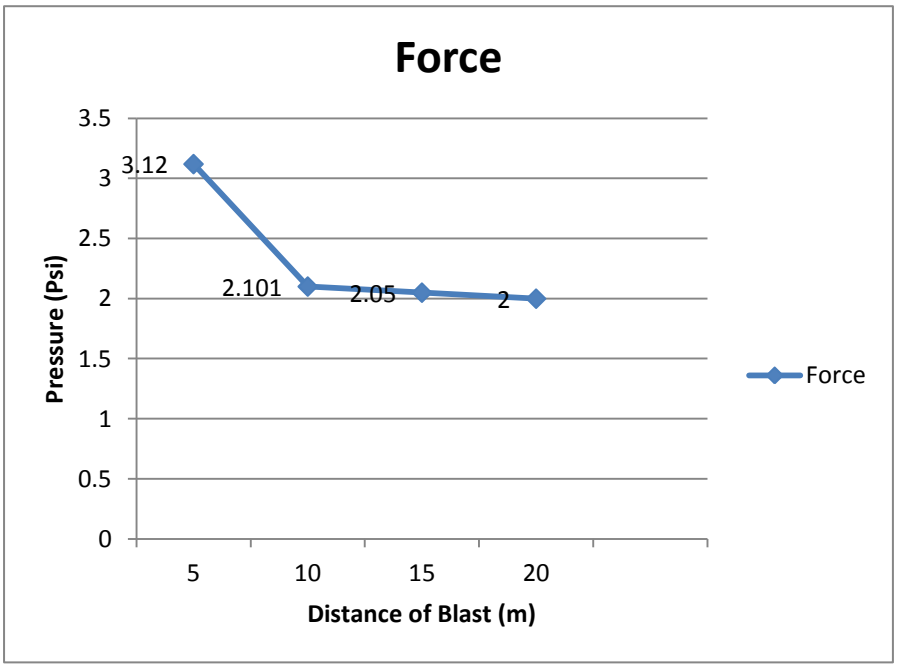


**FIG. 5 M The Graph showing Back pressure on the Building due to Blast**

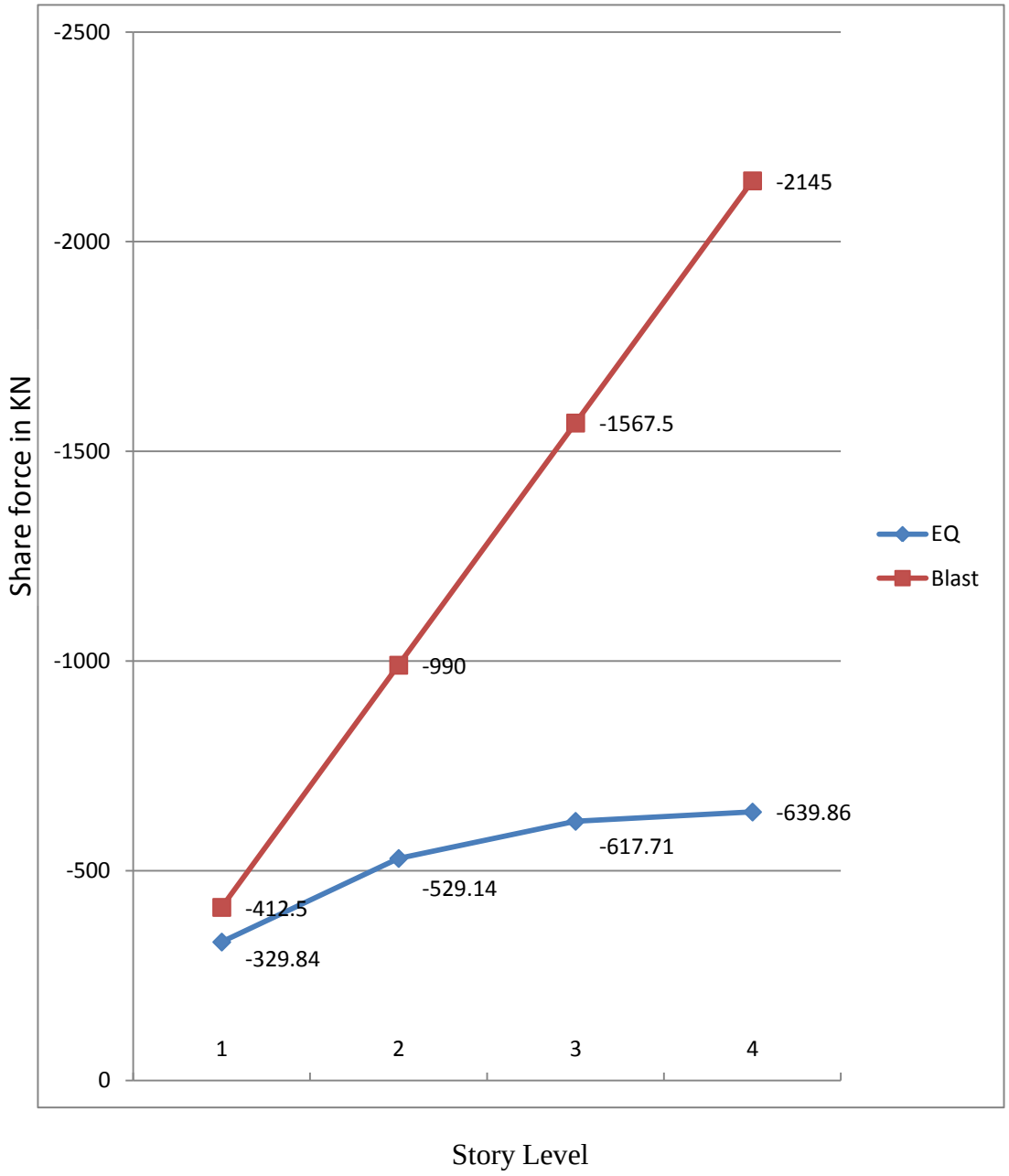


**FIG. 5 N Comparison of Shear Forces due to Blast Load and Earthquake Load**

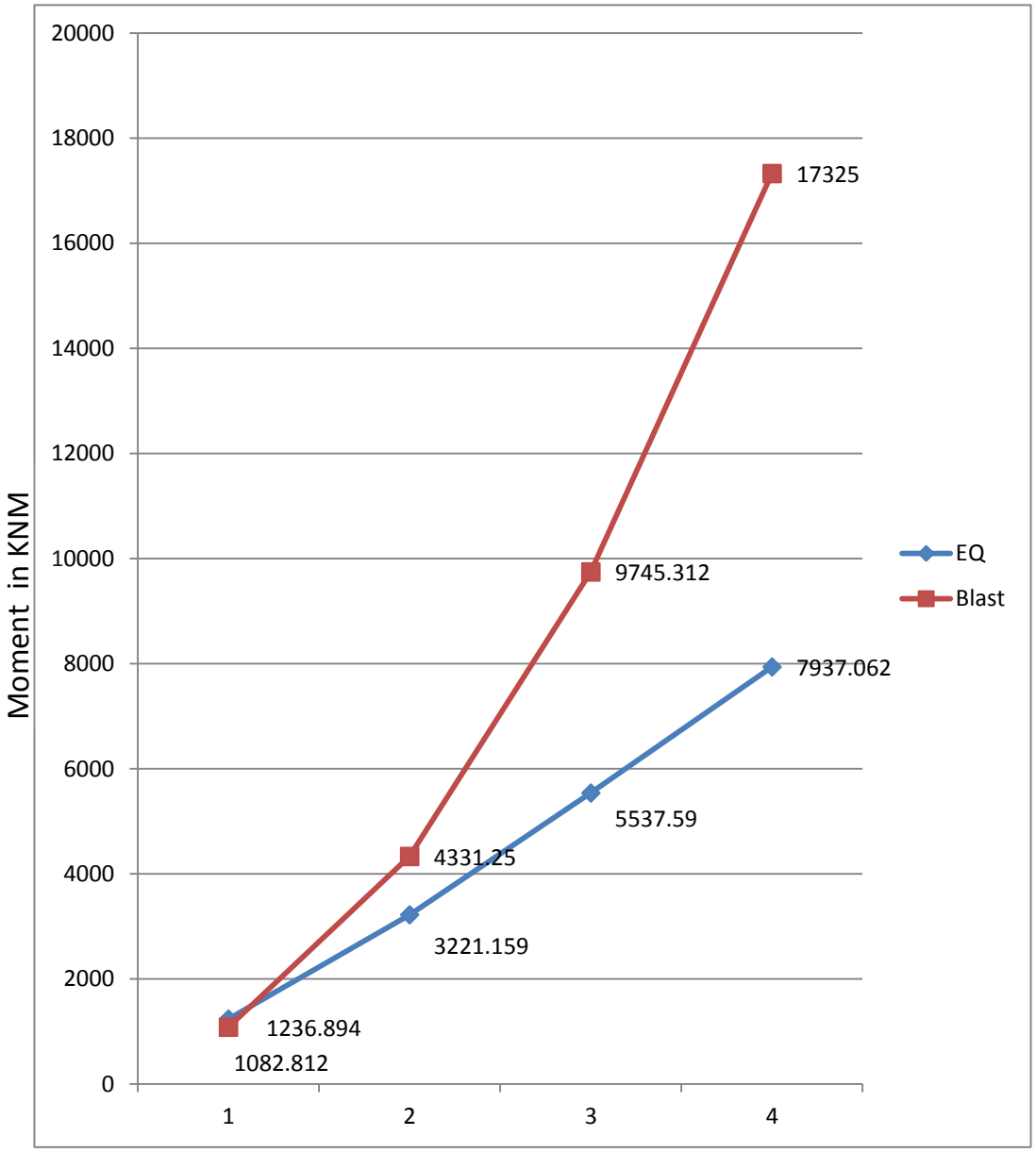


**FIG. 5 O Comparison of Moments due to Blast Load and Earthquake Load**

# CHAPTER 6

# CONCLUSIONS

## 1. CONCLUSION

For detail investigation of the performance of the building under blast loading, the first generation bench mark problem was considered. This was considered in order to verify the results viz response by comparing with standard results and to extrapolate the result for general structure. The blast loading was modeled using standard equations suggested by Smith et al. (1994 & 2001). Then influence of blast loading with variation of scale distanced was investigated.

The basic objective of the investigation is to study the effect of blasting loading on the bench mark problem of building by using ETABS as helping software for modeling the structure as well the performance of structure due to blast pressure was investigated by the standard equations apart from that influence of structural parameter investigated due blast pressure.

The following observations are noted during analysis of building by using E tabs software.

1. Effect of Blast Load decreases as Scaled distance increases.
2. The shear force and Moments are nearly 3.35 times more due to Blast load than Earthquake load.

## CHAPTER 7

## REFERENCES:


**1.** T. Ngo, P. Mendis, A. Gupta & J. Ramsay, " Blast Loading and Blast Effects on structure", The University of Melbourne, Australia, 2007.

**2.** TM 5-1300(UFC 3-340-02) U.S. Army Corps of Engineers (1990), "Structures to Resist the Effects of Accidental Explosions", U.S. Army Corps of Engineers, Washington, D.C., (also Navy NAVFAC P200-397 or Air Force AFR 88-22).

**3.** Kirk A. Marchand, Farid Alfawakhiri (2005), "Blast and Progressive Collapse" fact for Steel Buildings, USA.

**4.** D.L. Grote et al. (2001), "Dynamic behaviour of concrete at high strain rates and pressures", Journal of Impact Engineering, Vol. 25, Pergamon Press, NewYork, pp. 869-886

**5.** Demeter G. Fertis (1973), "Dynamics and Vibration of Structures", A Wiley-Interscience publication, pp. 343-434

**6.** Biggs, J.M. (1964), "Introduction to Structural Dynamics", McGraw-Hill, New York.

**7.** Risk Management Series,FEMA428,EXPLOSIVE BLAST,2003,Chapter four,www.fema.gov.

**8.** Risk Management series(2003)FEMA427,Primer for Design of Commercial Buildings to Mitigate terrorist attacks,www.fema.gov.

**9.** Chengqing Wu and Hong Ho(2007),Numerical simulation of structural response and damage to simultaneous ground shock and airblast loads,International Journal of Impact Engineering,34,556-572.

**10.** Asasaa B.M. Luccioni,R.D.Ambrosini and R.F. Danesi(2003),Analysis of Building Collapse under Blast loads B.M. Luccioni,26,63-71

**11.** Mays GC and Smith PD (2001) Blast Effects on Buildings, Cranfield University

**12.** IS 4996:1968, (1993) "Indian Standard Criteria for Blast Resistant Design of Structures of Explosion above Ground", Bureau of Indian Standards, New Delhi, India.

**13.** TM 5-1300, (1990) "The Design of Structures to Resist the Effects of Accidental Explosions", Technical Manual, US Department of the Army, Navy and Air Force, Washington DC, USA.